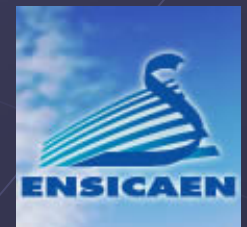


Classical Texture Analysis

D. Chateigner

*CRISMAT-ENSICAEN; IUT-UCBN
6 bd. M. Juin 14050 Caen*



Outline

Qualitative aspects of crystallographic textures

Grains, Crystallites and Crystallographic planes

Normal diffraction

Effects on diffraction diagrams, their limitations

θ - 2θ scans

Asymmetric scans

ω -scans (rocking curves)

Representations of texture: pole figures

Pole Sphere

Stereographic projection

Equal-area projection: Lambert/Schmidt projection

Pole figures

Localisation of crystallographic directions from pole figures

Direct and normalised pole figures

Normalisation

Incompleteness and corrections of pole figures

Single texture component

Multiple texture components

Pole figures and (hkl) multiplicity

A real example

Pole figure types

- Random texture

- Planar textures

- Fibre textures

- Three-dimensional texture

Pole Figures and Orientation spaces

- Mathematical expression of diffraction pole figures and ODF

- From pole figures to the ODF

- Orientations g and pole figures

- Euler angle conventions

- From $f(g)$ to pole figures

- Deal with ODF in the ψ space

- Plotting the ODF

Inverse pole figures

ODF refinement

- Generalised spherical harmonics

- WIMV

- Entropy modified WIMV and Entropy maximisation

- ADC, Vector and component methods

- ODF coverage

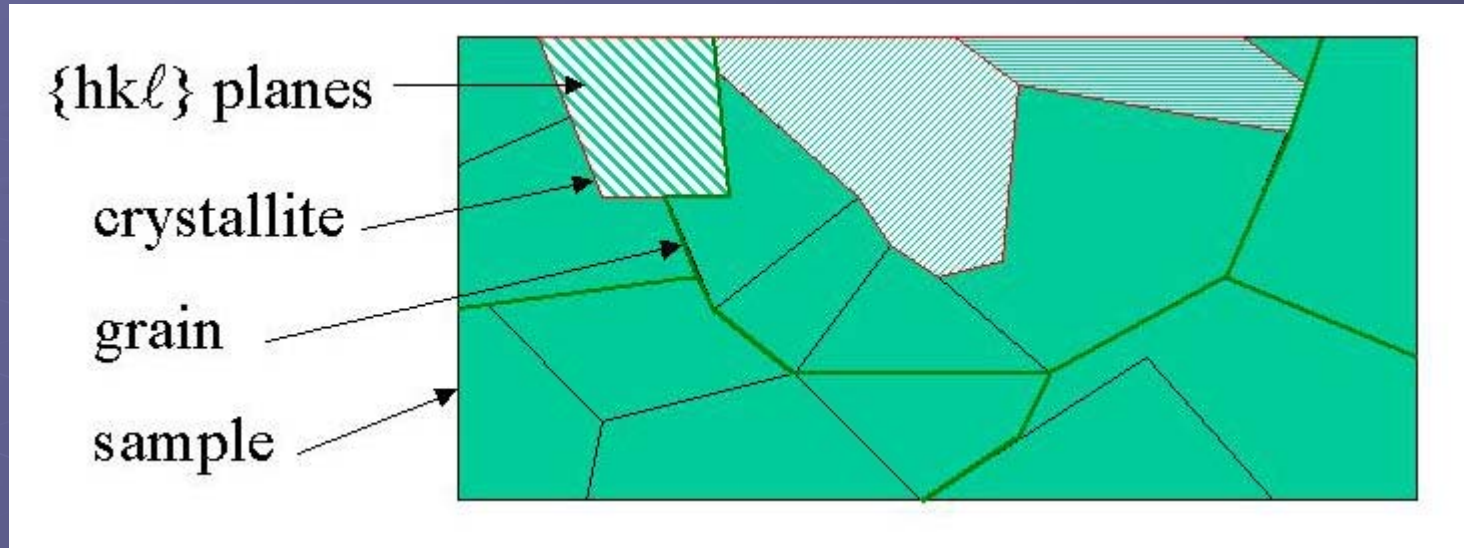
- Reliability and texture strength estimators

Why needing Combined analysis

Qualitative aspects of texture

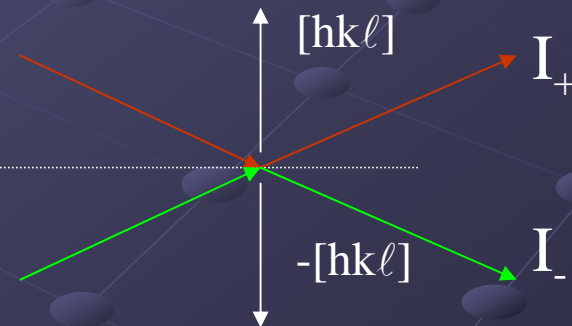
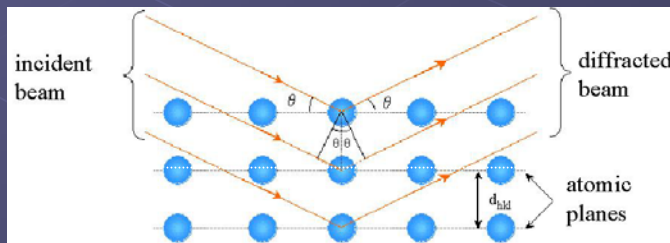
- Polycrystal: aggregate of grains, different phases, sizes, shapes, orientations ...
- Diffraction:
 - probes lattice planes: crystallites, not grains
 - x-rays, neutrons or electrons
- SEM:
 - grains, not crystallites (coherent, single crystal domains)
 - shape vs crystallographic texture (EBSD)

Grains, crystallites, crystallographic planes



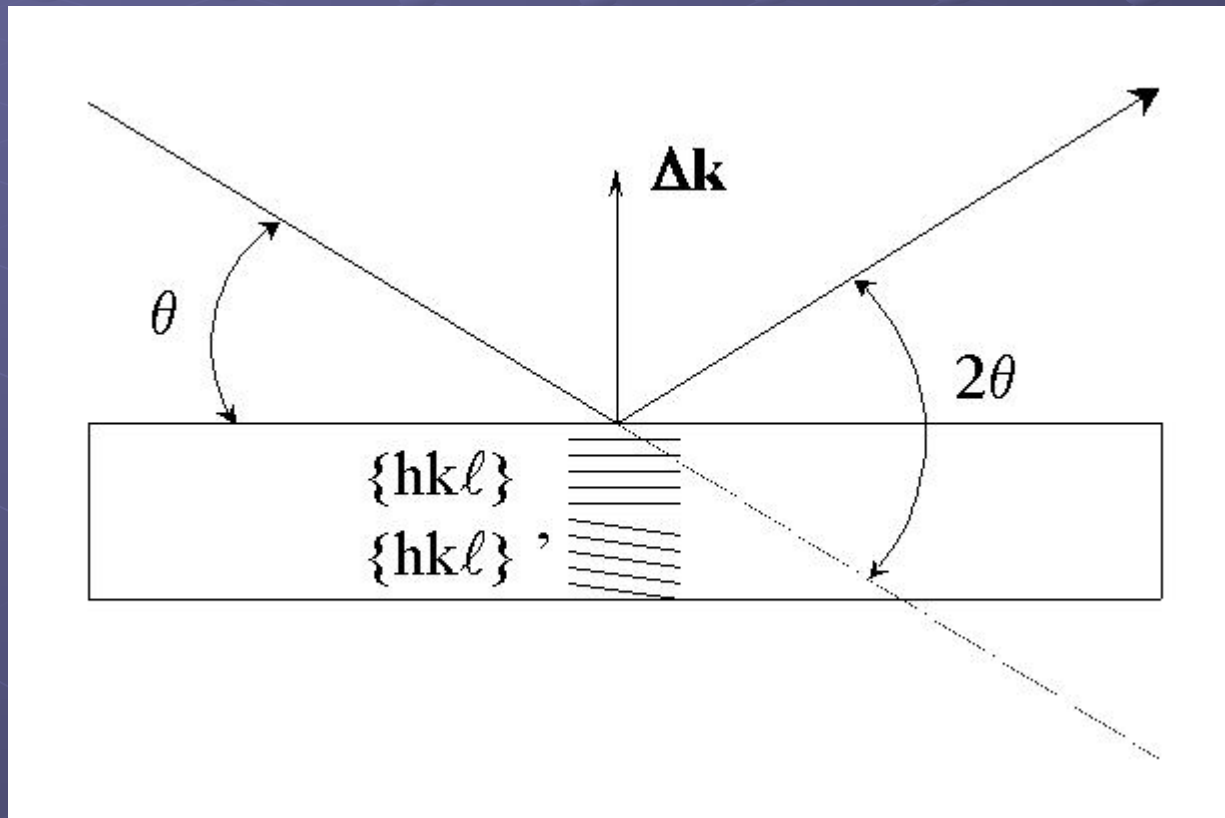
Friedel's law:

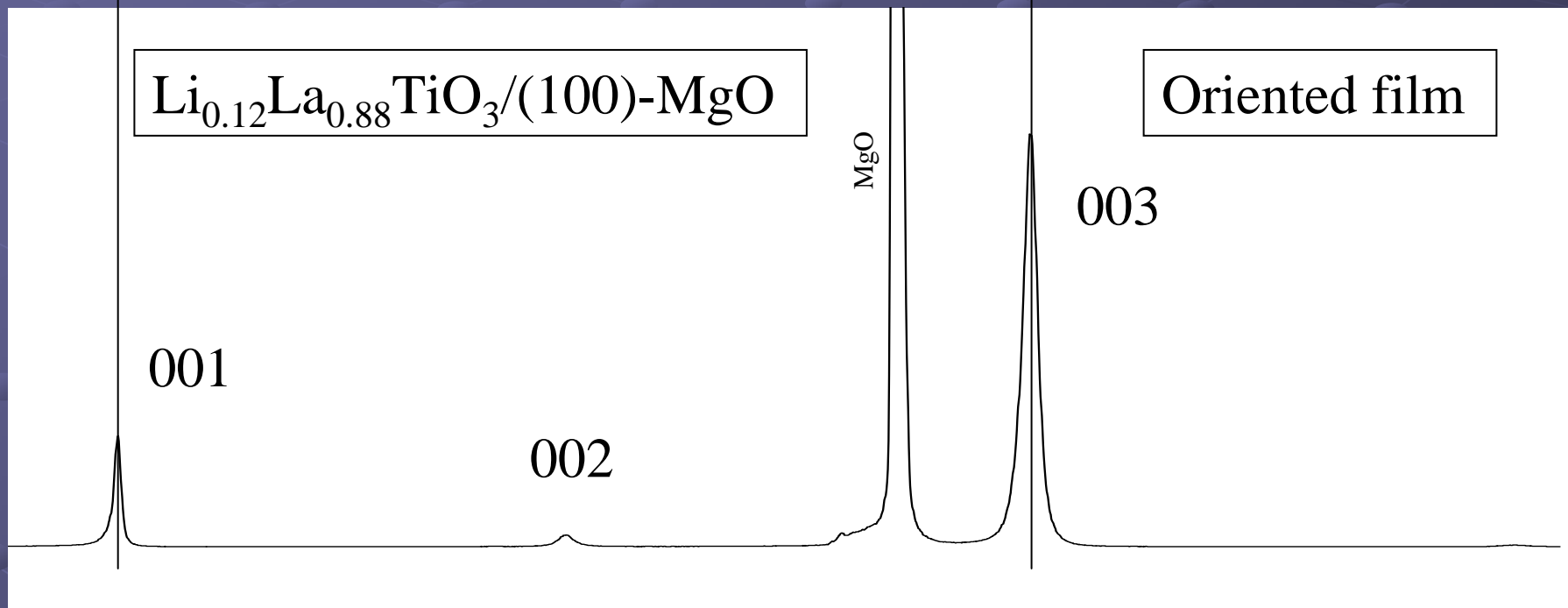
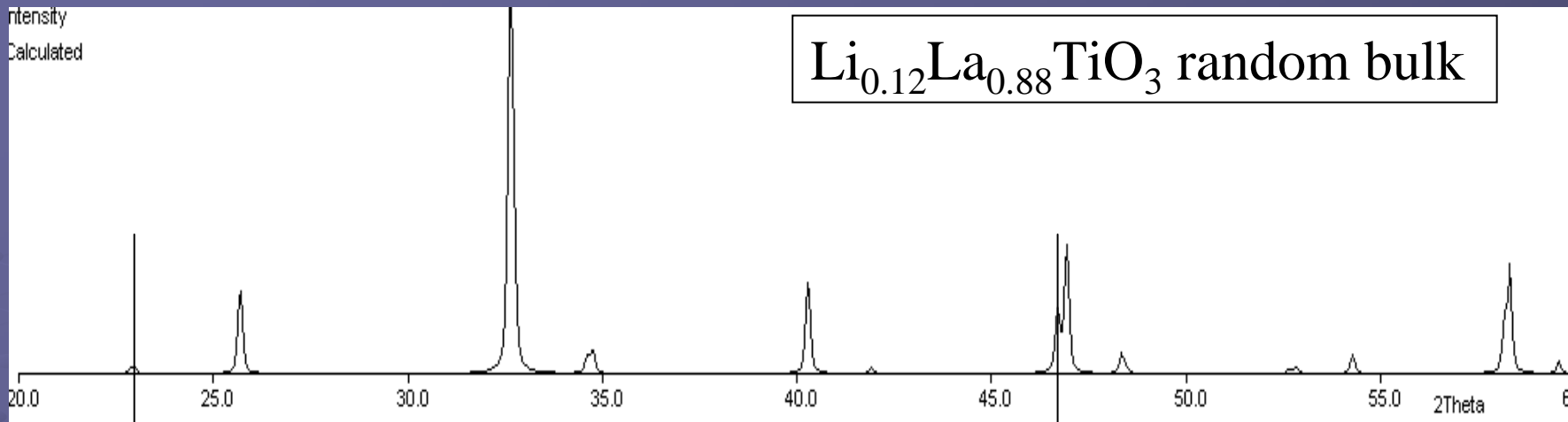
$I_{hkl} = I_{-h-k-l}$ using normal diffraction
+ or - directions not distinguished



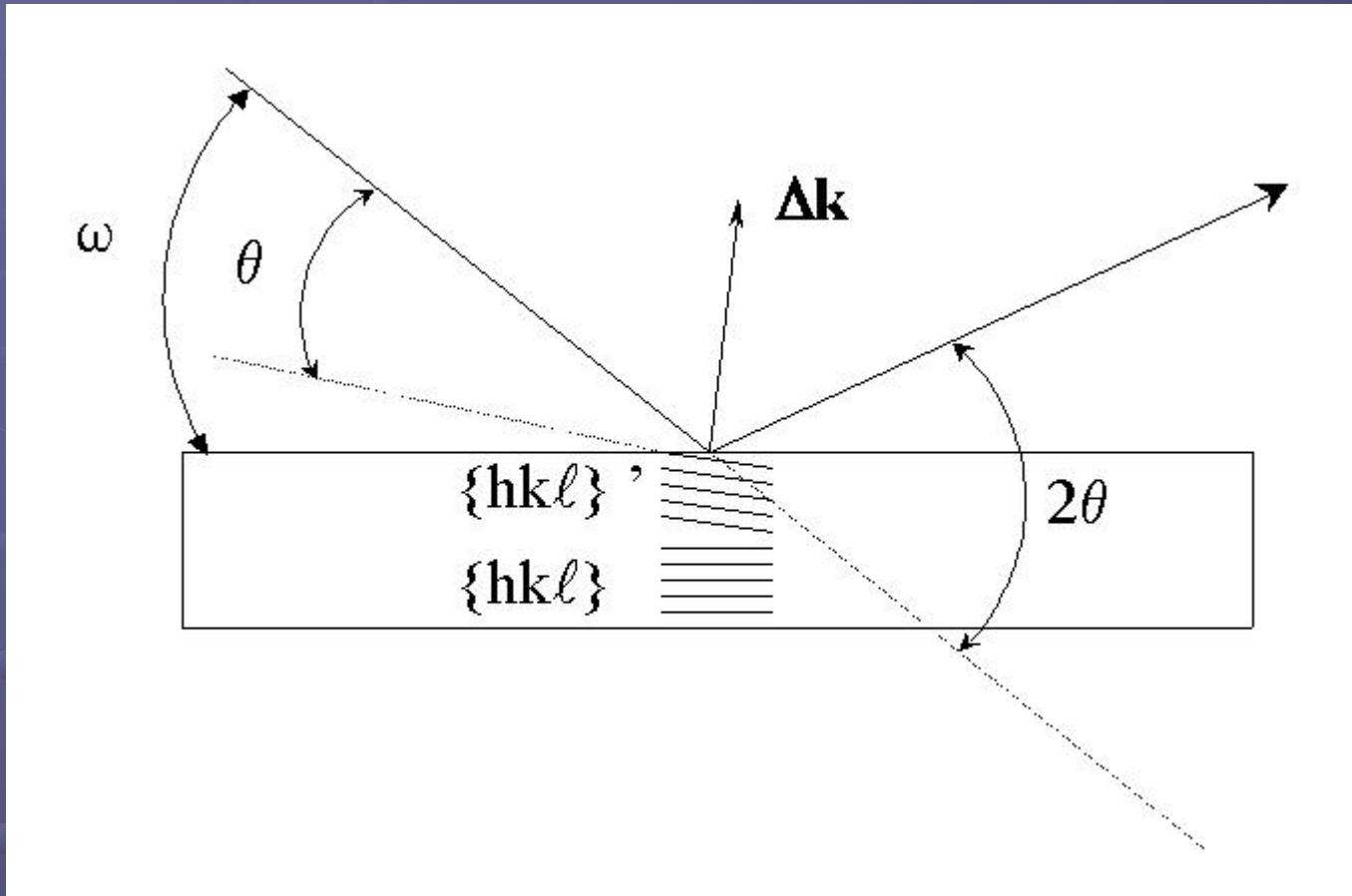
Texture effects on diffraction diagrams

θ - 2θ scan: probes only parallel planes

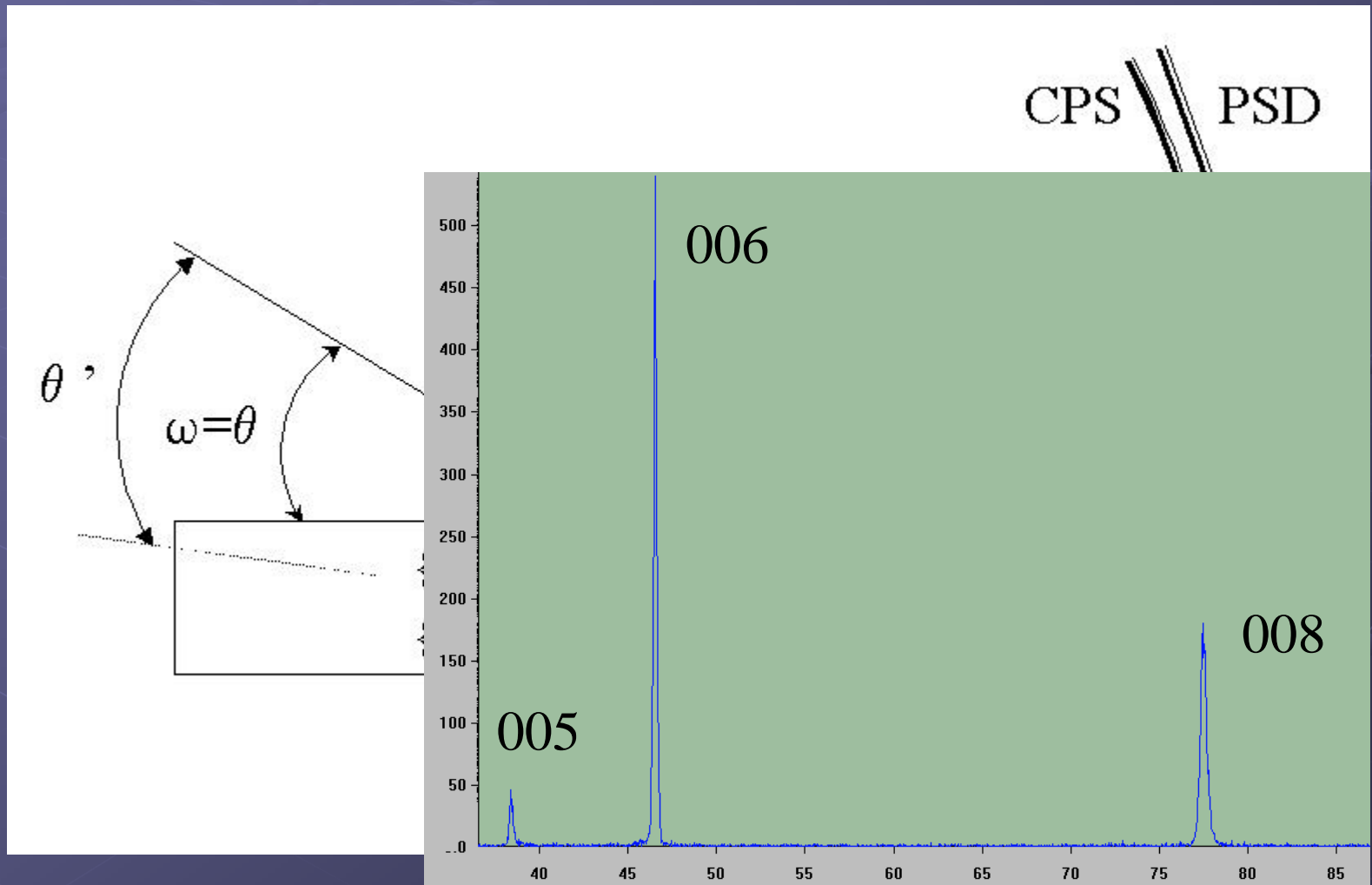




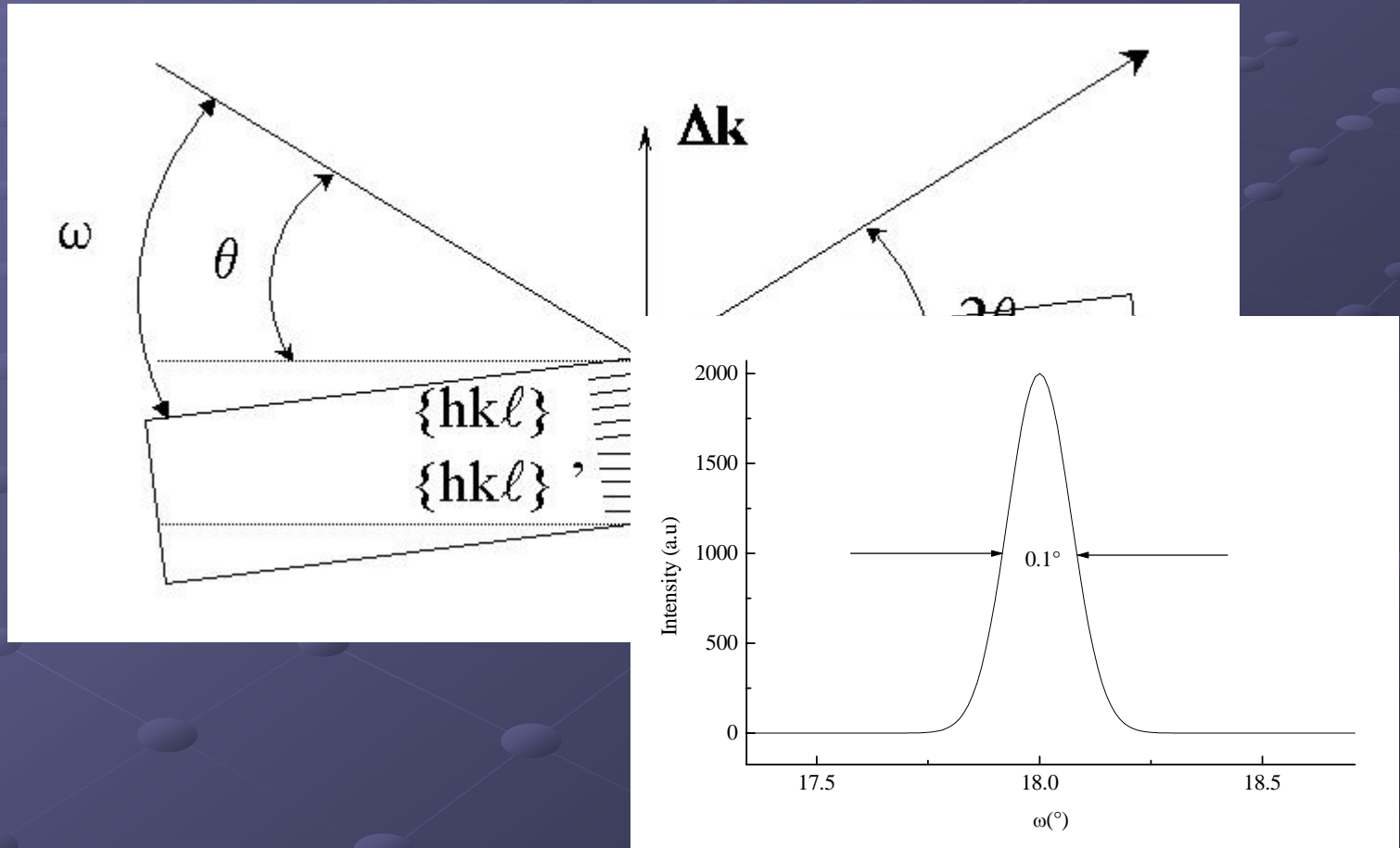
asymmetric scan: probes only inclined planes



mixed scan: probes specific planes for
specific orientations

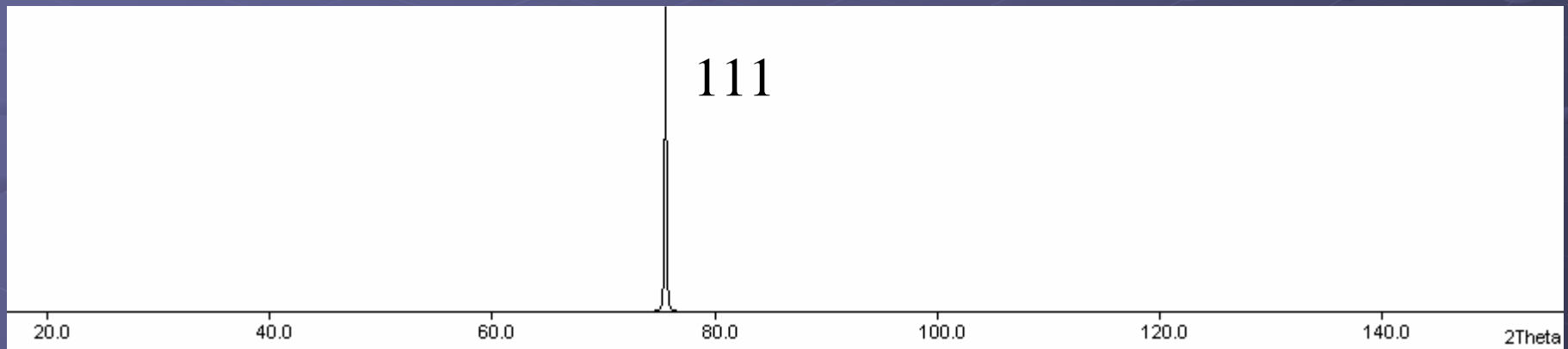


ω scan: probes orientation of only one plane type (fixed θ), only for small ω - θ



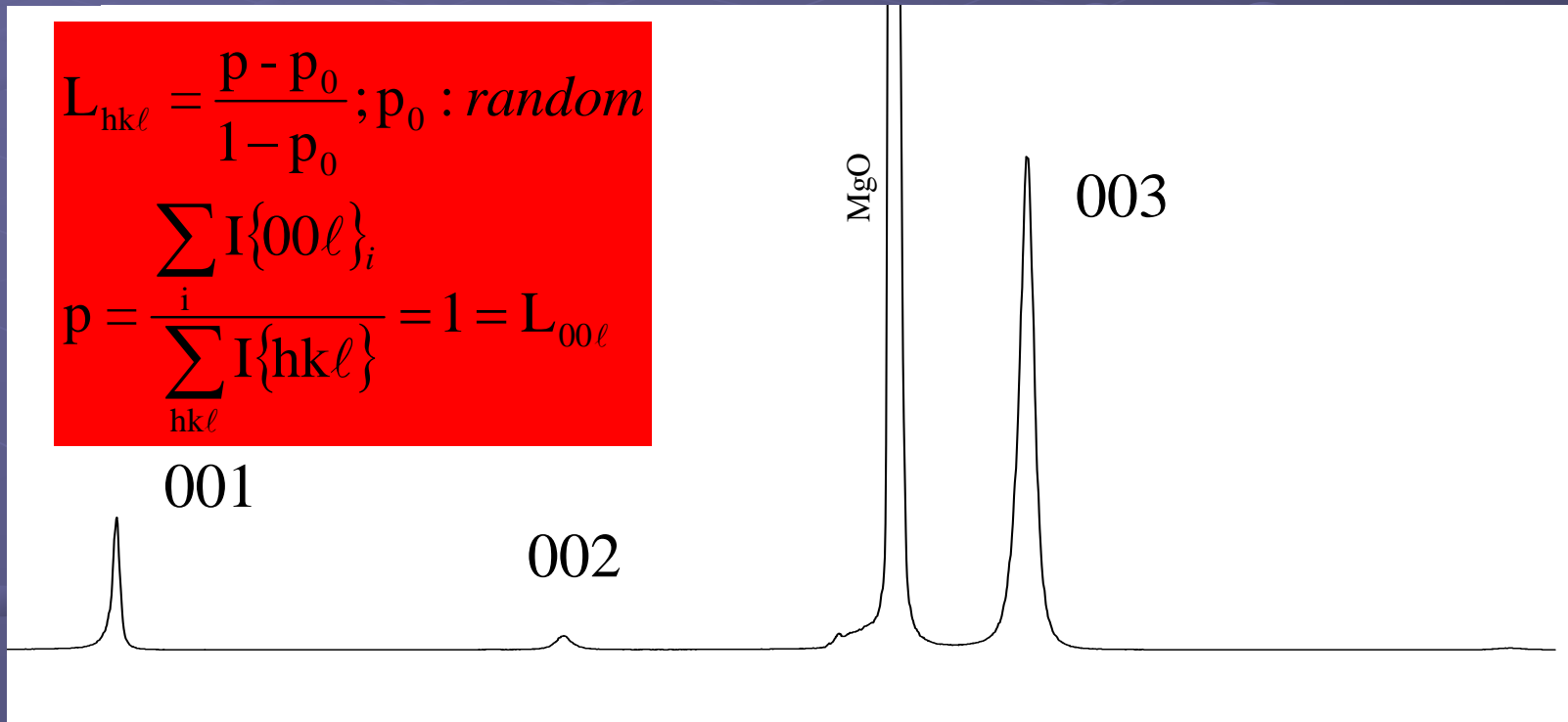
limitations: available θ (or other) range

diamond (Fd3m), 2.52 Å neutrons, up to $2\theta = 150^\circ$

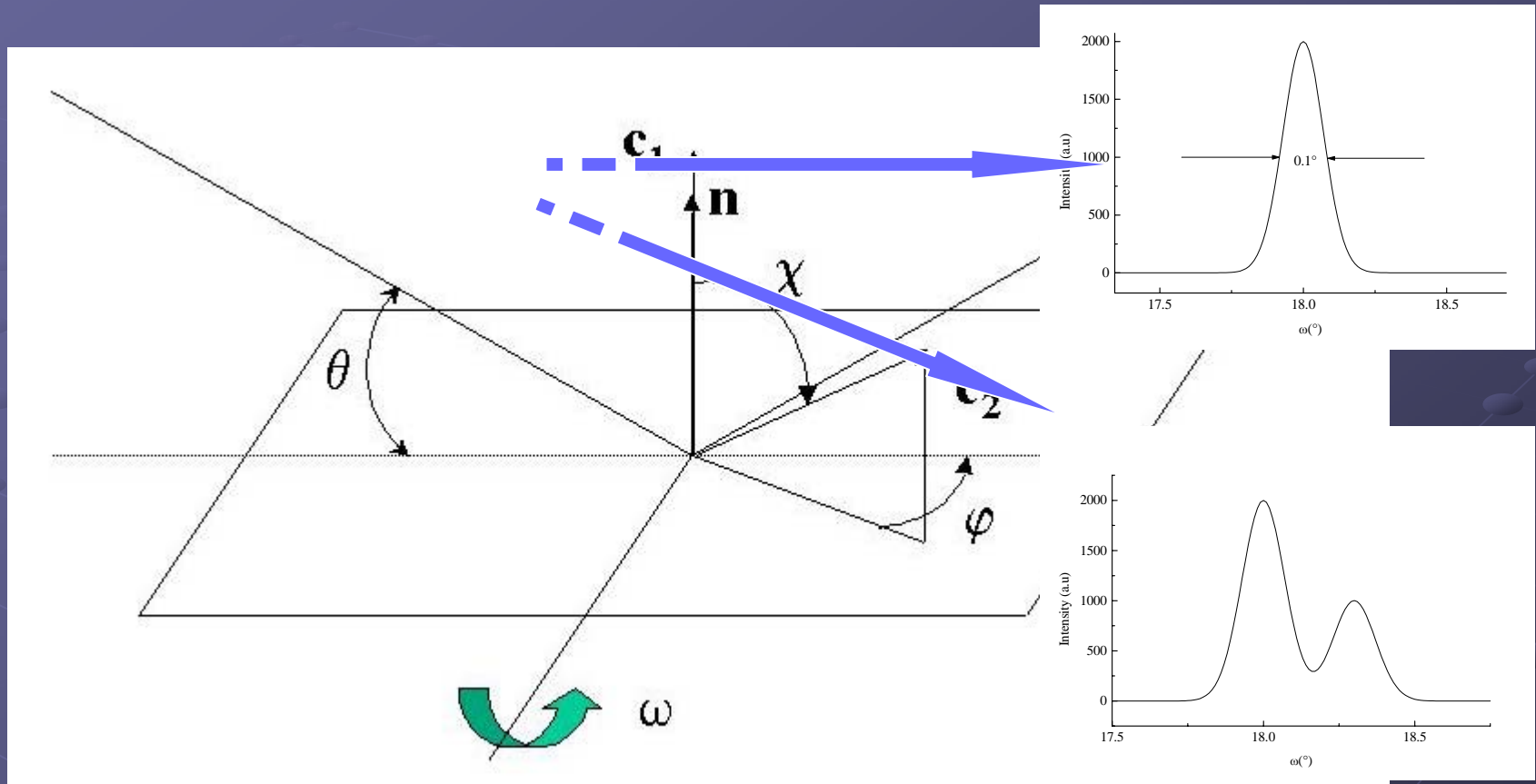


limitations: 2 texture components

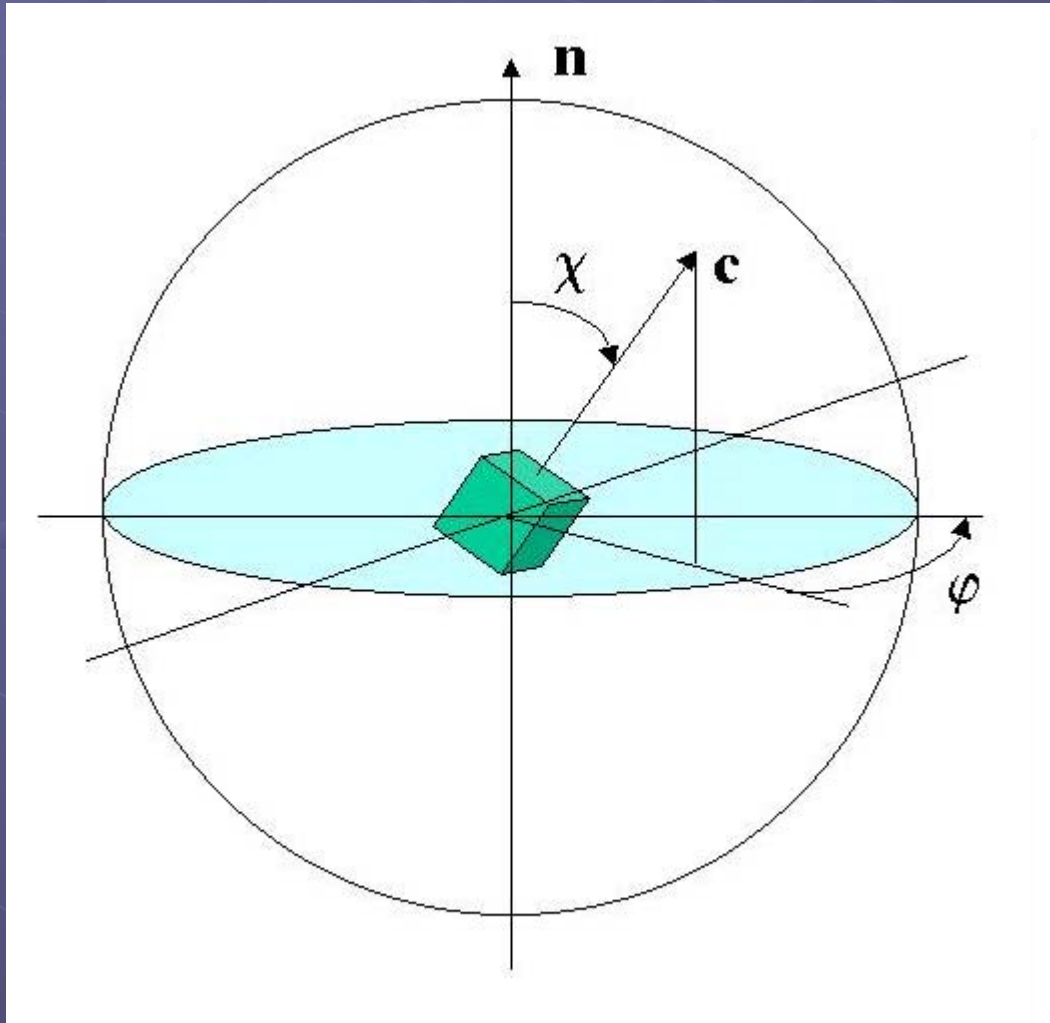
same c-axes direction, but not same a



limitations: 2 texture components, one inclined



Representations of texture: pole figures



One crystallite oriented
in the Pole sphere:

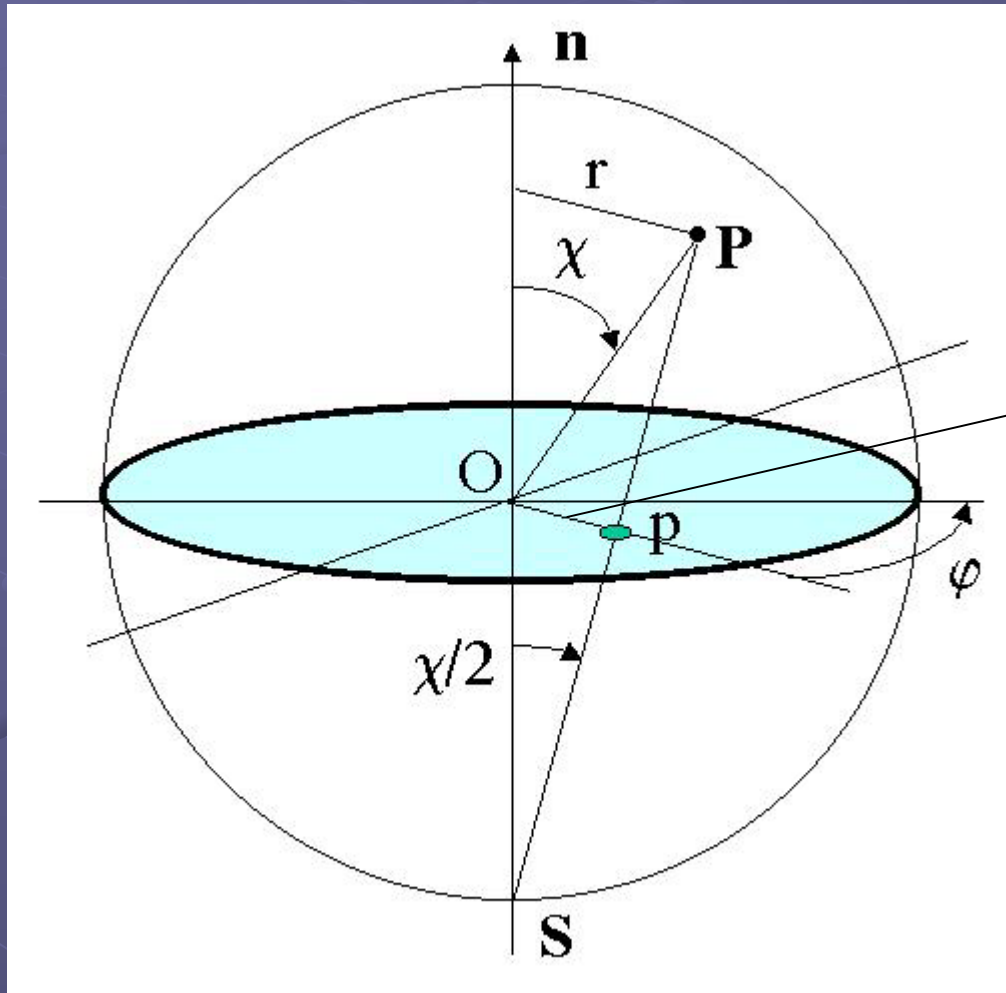
- location of all
 $[hkl] \in$ unit sphere

- $dS = \sin\chi \, d\chi \, d\phi$

- (χ, ϕ) : angles in the
diffractometer space ♠

Hard to visualise: needs
pole figures

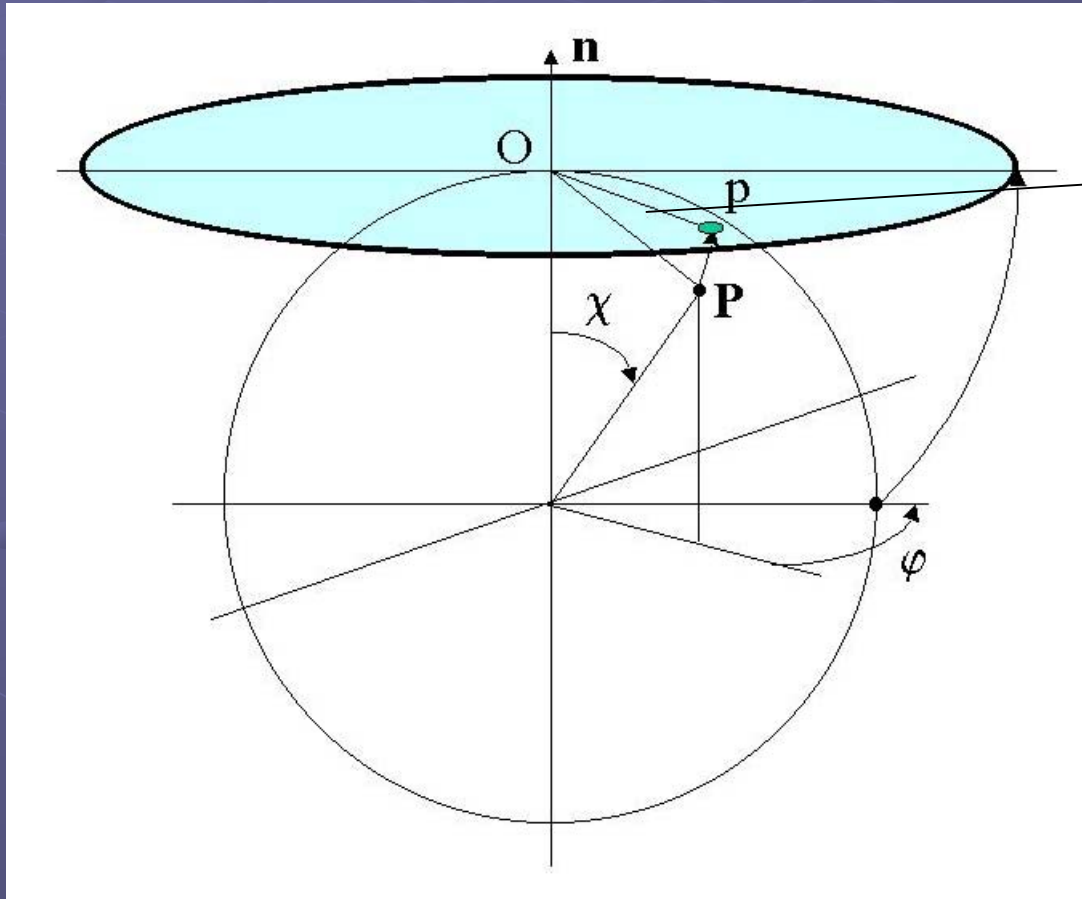
Stereographic projections: equal angle



Poles: $p(r', \phi)$:

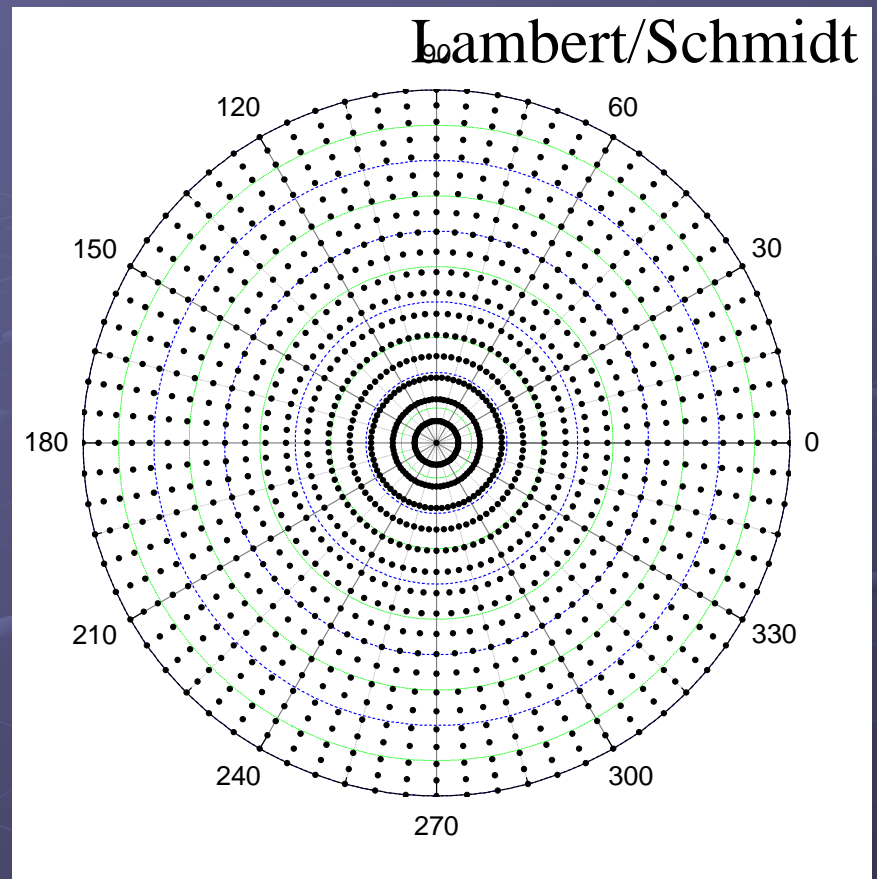
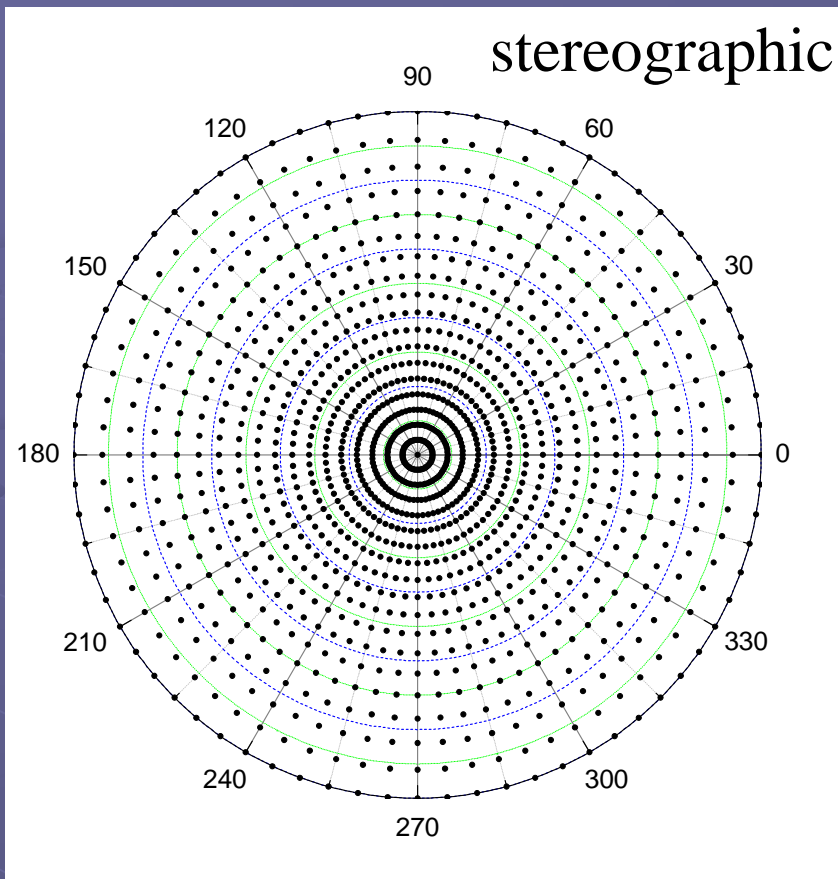
$$r' = R \tan(\chi/2)$$

Lambert projections (equal area)



Poles: $p(r', \phi)$:

$$r' = 2R \sin(\chi/2)$$

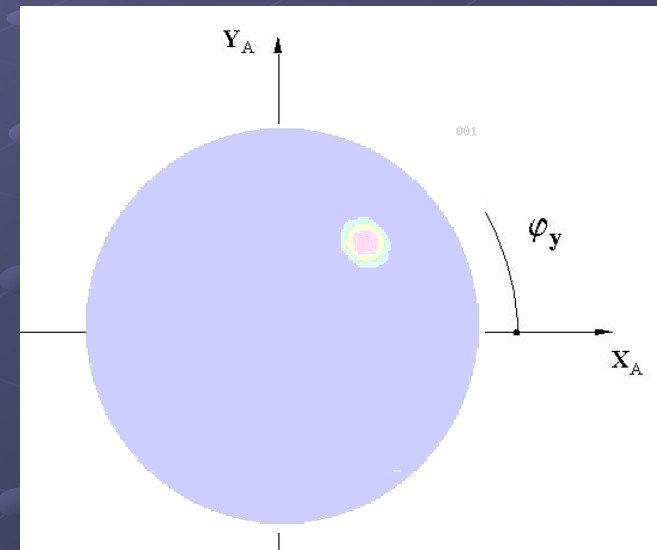
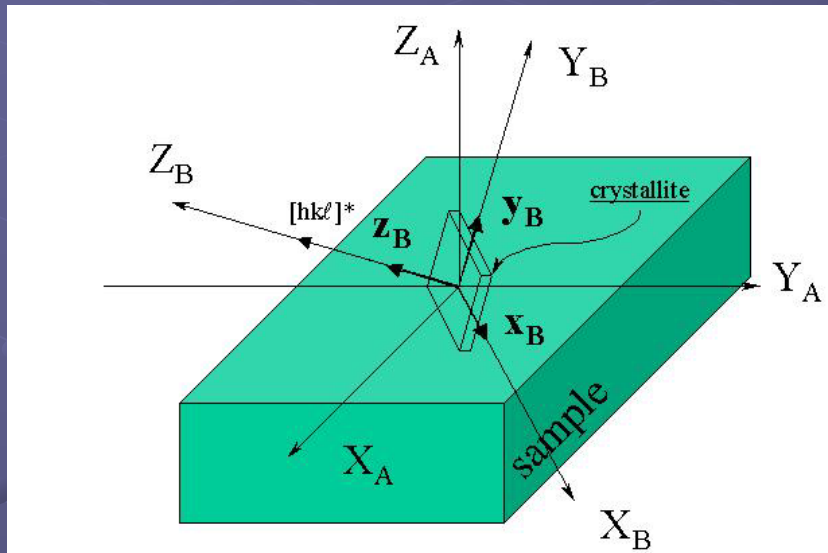


$5^\circ \times 5^\circ$ grid: 1368 points

Pole figures

$\{hkl\}$ -Pole figure: location of distribution densities, for the $\{hkl\}$ diffracting plane, defined in the crystallite frame K_B , relative to the sample frame K_A .

Pole figures space: $\hat{\Delta}$, with $\mathbf{y} = (\vartheta_y, \varphi_y) = [hkl]^*$

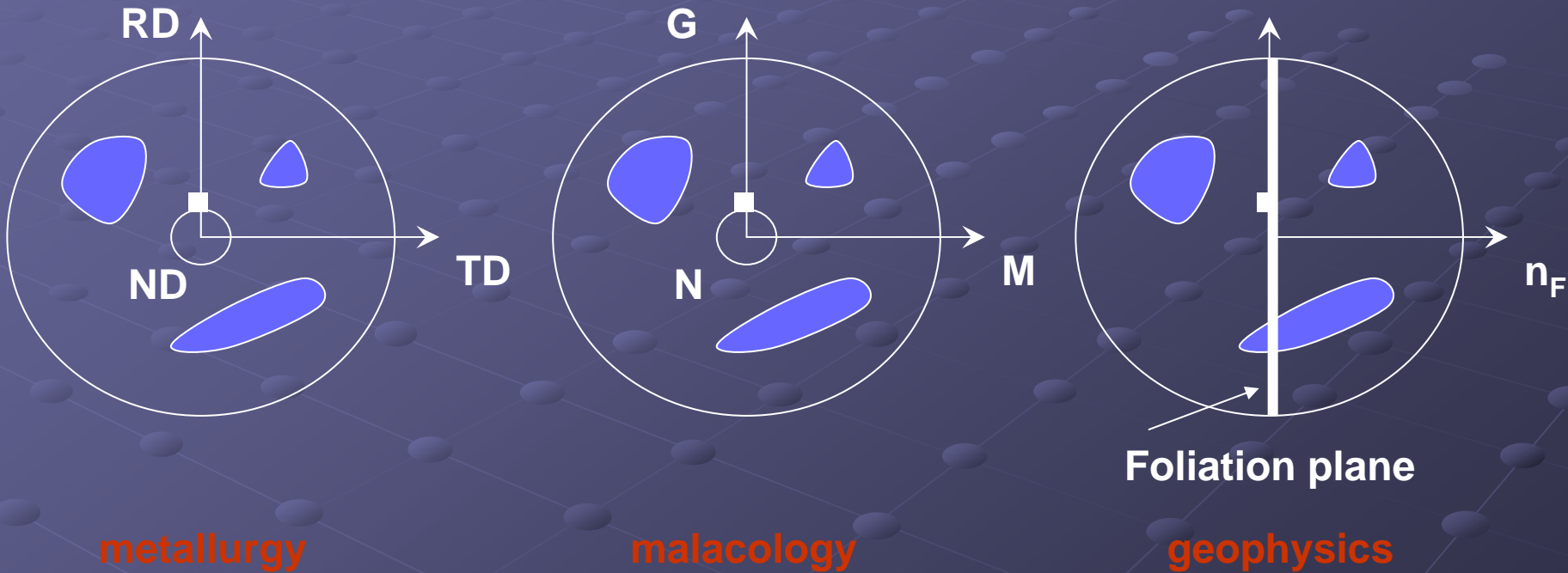


Direct Pole Figure: built on diffracted intensities $I_h(\mathbf{y})$, $\mathbf{h} = \langle hkl \rangle^*$

Normalised Pole Figure: built on distribution densities $P_h(\mathbf{y})$

Density unit: the "multiple of a random distribution", or "m.r.d."

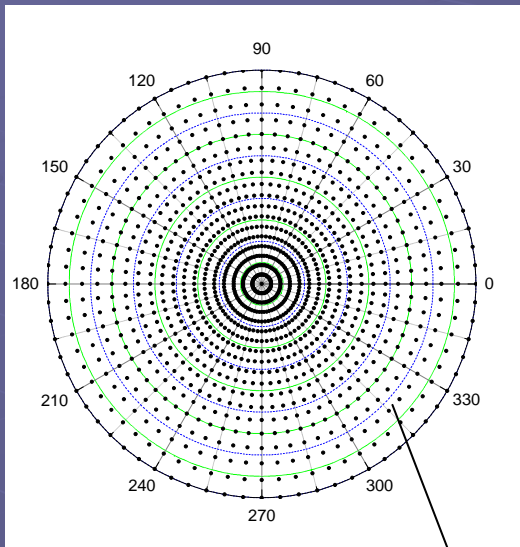
Usual pole figure frames K_A



Thin films: substrate directions ...

X_A, Y_A, Z_A

Normalisation



$$I_{\mathbf{h}}(\vartheta_y, \varphi_y)$$

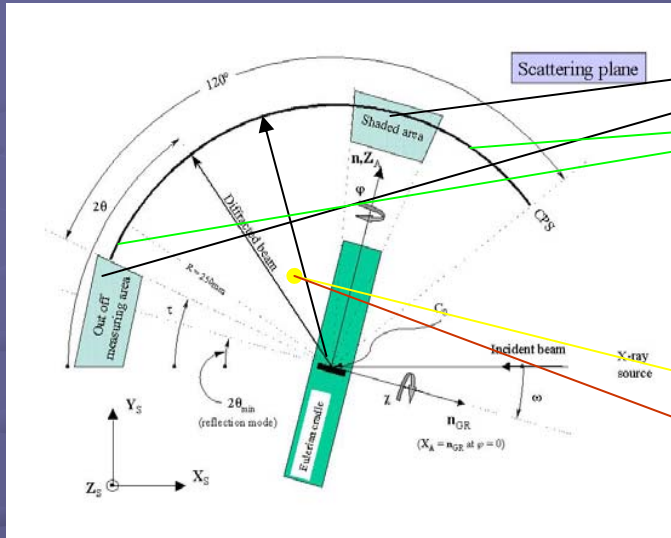
$$I_{\mathbf{h}}^{\text{total}} = \int_{\varphi_y=0}^{2\pi} \int_{\vartheta_y=0}^{\pi/2} I_{\mathbf{h}}(\vartheta_y, \varphi_y) \sin \vartheta_y \, d\vartheta_y \, d\varphi_y$$

$$I_{\mathbf{h}}^{\text{random}} = I_{\mathbf{h}}^{\text{total}} / \int_{\varphi_y=0}^{2\pi} \int_{\vartheta_y=0}^{\pi/2} \sin \vartheta_y \, d\vartheta_y \, d\varphi_y$$

$$P_{\mathbf{h}}(\mathbf{y}) = \frac{I_{\mathbf{h}}(\mathbf{y})}{I_{\mathbf{h}}^{\text{random}}}$$

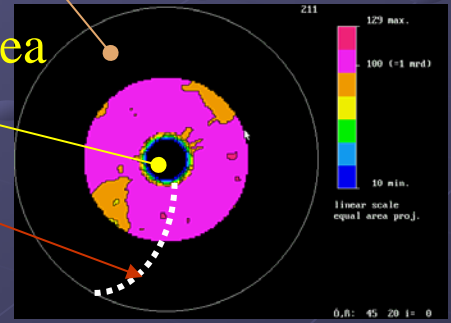
- Only valid for complete pole figures:
 - neutrons in symmetric geometry
- Needs a refinement strategy to get I^{random} for all \mathbf{h} 's

Incompleteness and corrections of pole figures

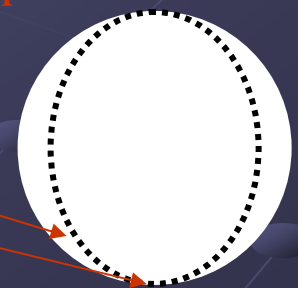
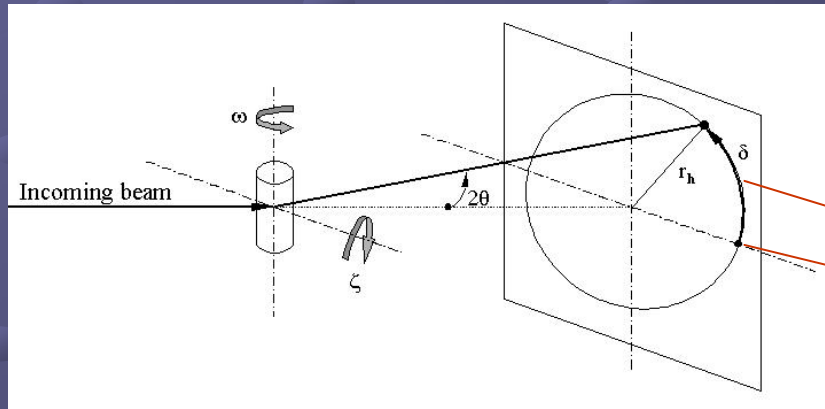


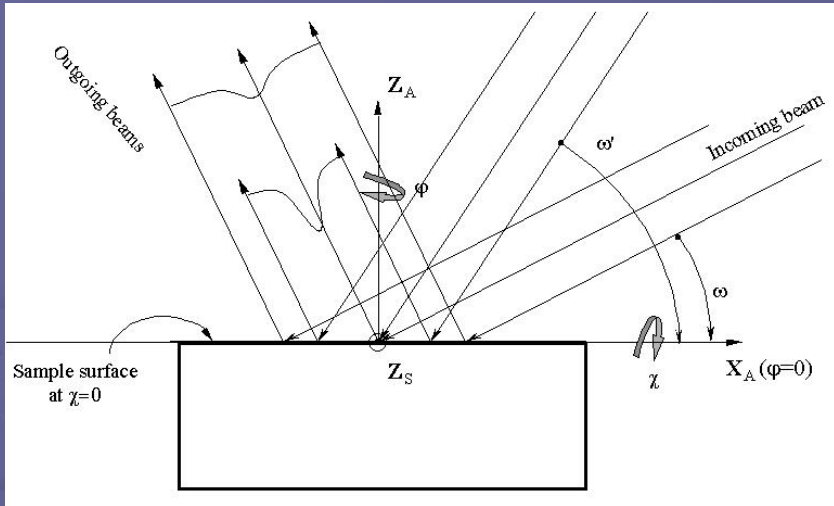
Missing Bragg peaks
 Absorption + volume
 Defocusing (x-rays)

Blind area

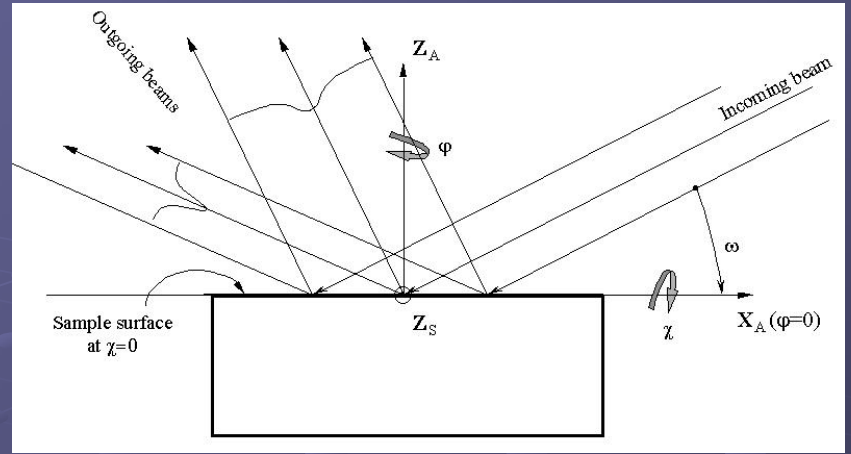


Localisation

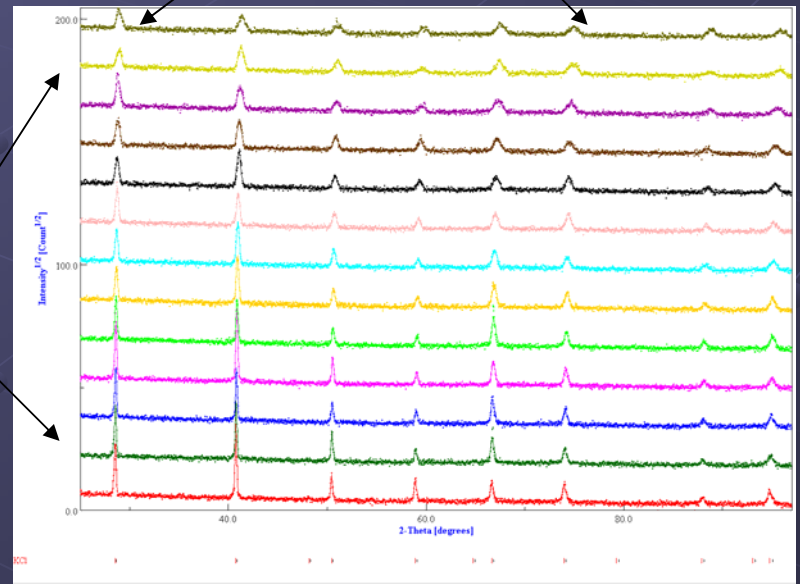
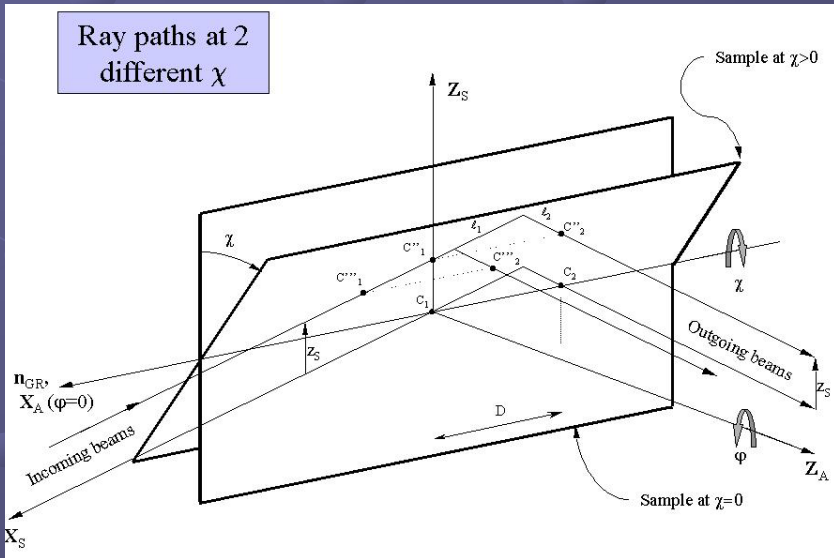




ω -defocusing
 χ -defocusing



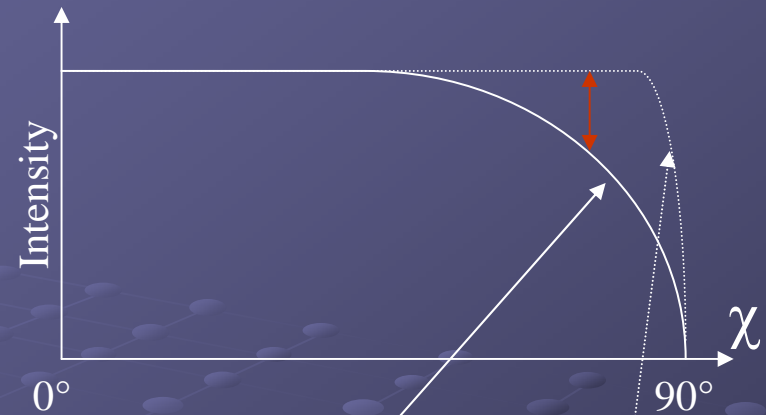
2θ -defocusing



Defocusing corrections:

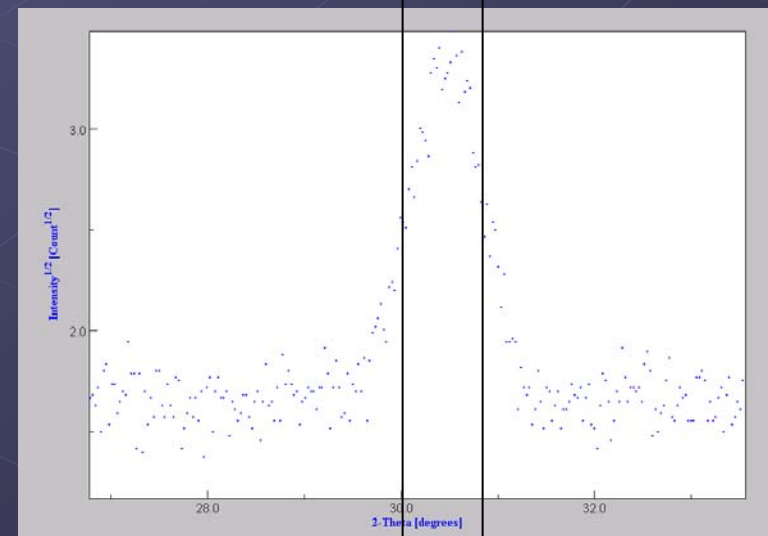
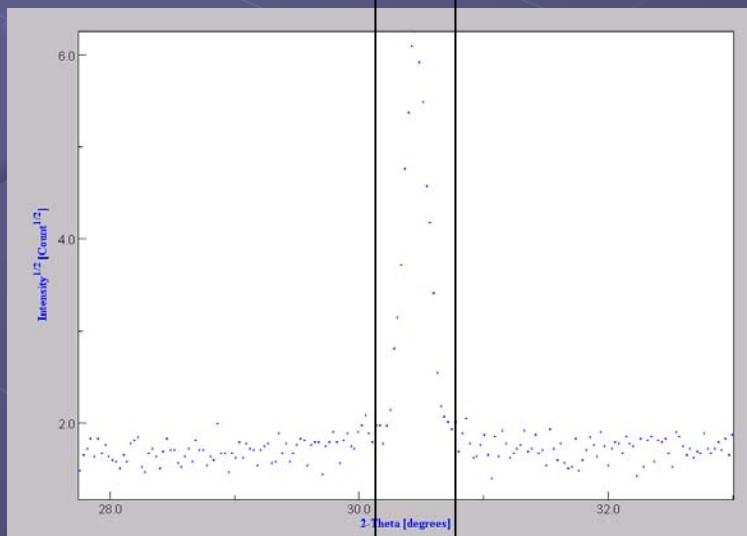
- Calibration on a random powder

$$\begin{aligned}
 I_{\chi,\omega,\theta}^{\text{cor}} &= I_{\chi,\omega,\theta}^{\text{meas}} \frac{I_{0,\omega,\theta}^{\text{rand}}}{I_{\chi,\omega,\theta}^{\text{rand}}} && \text{Net intensities} \\
 &&& \text{(point detector)} \\
 &= \left[I_{\chi,\omega,\theta}^{\text{meas}} - I_{0,\omega,\theta}^{\text{bkg}} \frac{I_{\chi,\omega,\theta}^{\text{bkg}}}{I_{0,\omega,\theta}^{\text{bkg}}} \right] \frac{I_{0,\omega,\theta}^{\text{rand}} - I_{0,\omega,\theta}^{\text{bkg}}}{I_{\chi,\omega,\theta}^{\text{rand}} - I_{0,\omega,\theta}^{\text{bkg}}}
 \end{aligned}$$

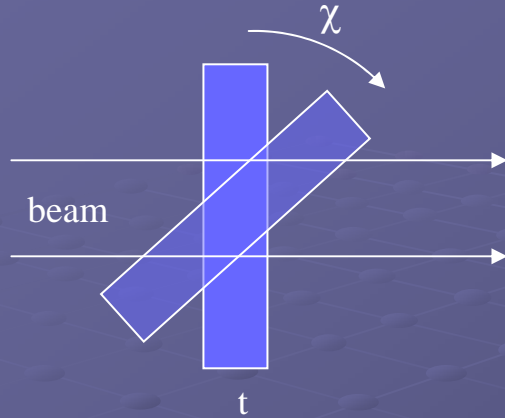


Peak maximum (point detector)
 Integrated intensity (1D or 2D detector)

- Total integration of the peak (direct integration or fit)



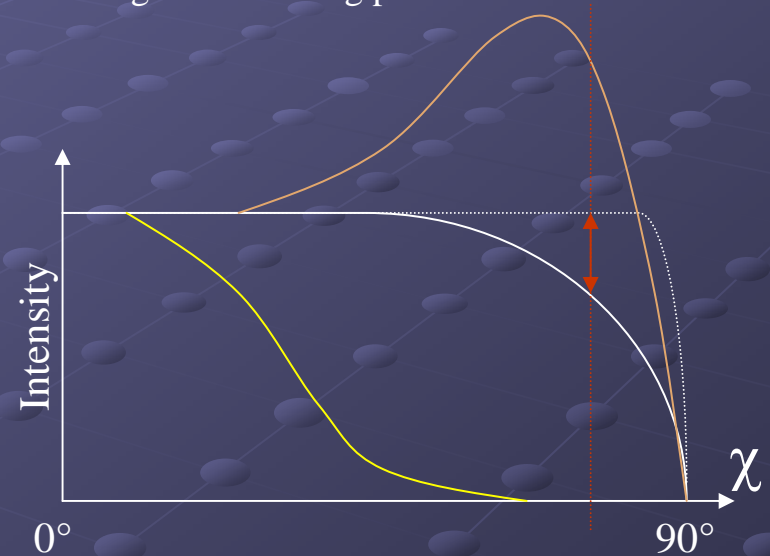
Absorption/Volume corrections:



Specific to each instrumental geometry
 Sample dependent (films, multilayers ...)
 Modifies the defocusing curves
 Can be integrated in fitting procedures

Top film

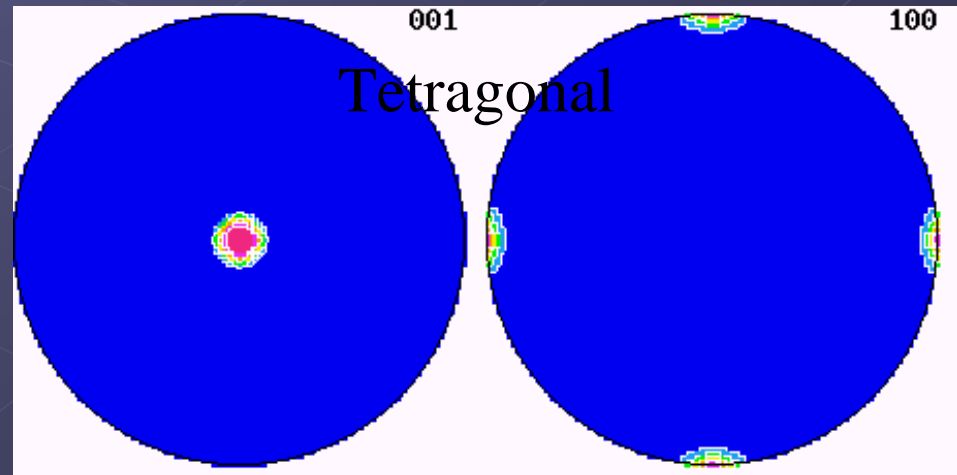
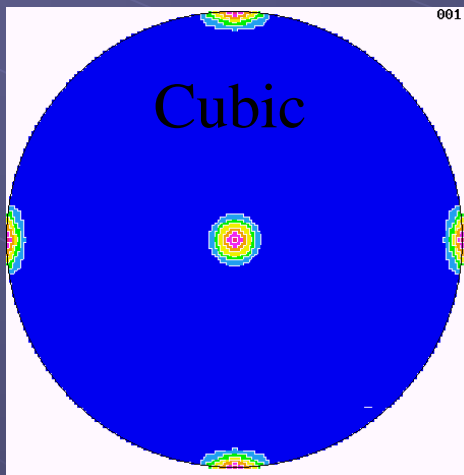
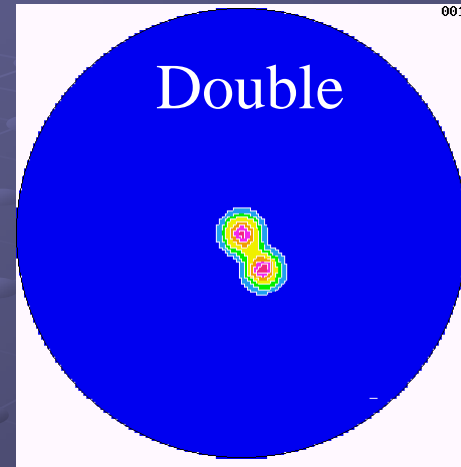
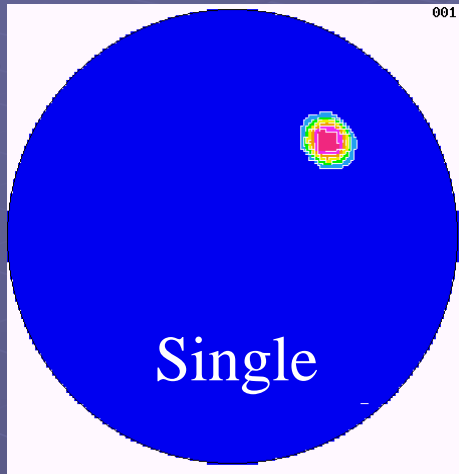
$$I(0) = I(\chi) \frac{(1 - \exp(-2\mu T / \sin \theta_i))}{(1 - \exp(-2\mu T / \sin \theta_i \cos \chi))}$$



Covered layer

$$I(0) = I(\chi) \frac{(1 - \exp(-2\mu T / \sin \theta_i)) \exp\left(\frac{-2\sum_j \mu_j T_j}{\sin \theta_i}\right)}{(1 - \exp(-2\mu T / \sin \theta_i \cos \chi)) \exp\left(\frac{-2\sum_j \mu_j T_j}{\sin \theta_i \cos \chi}\right)}$$

Single or multiple texture components, multiplicity



Program convention !

Pole figure test file: test5572

points in (φ_y, θ_y) :

(0,0)

(0,10)

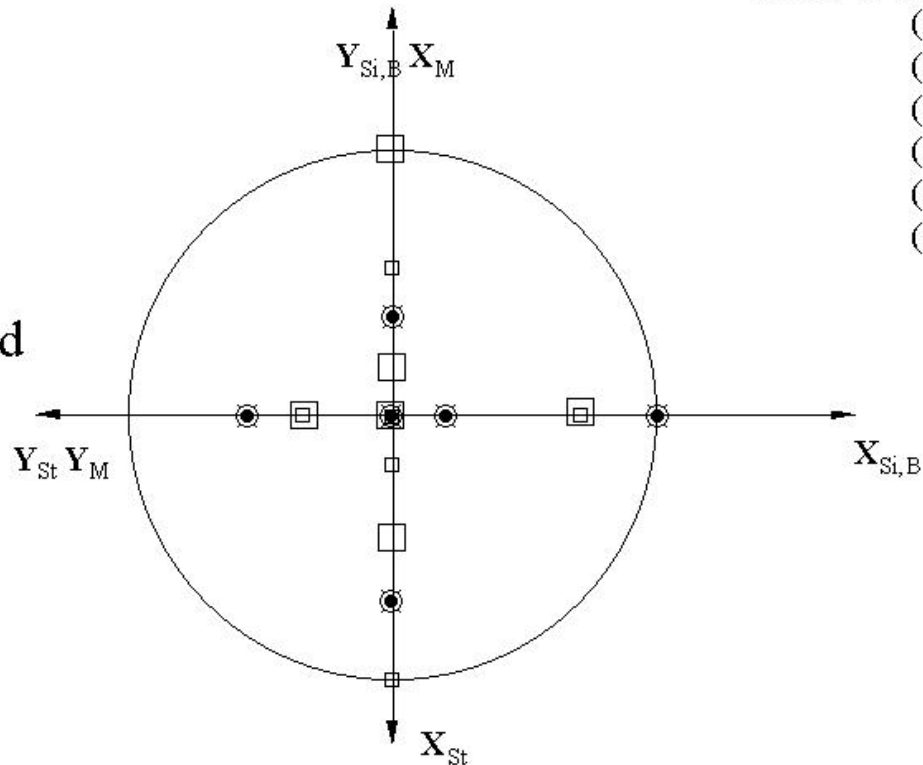
(90,30)

(180,50)

(270,70)

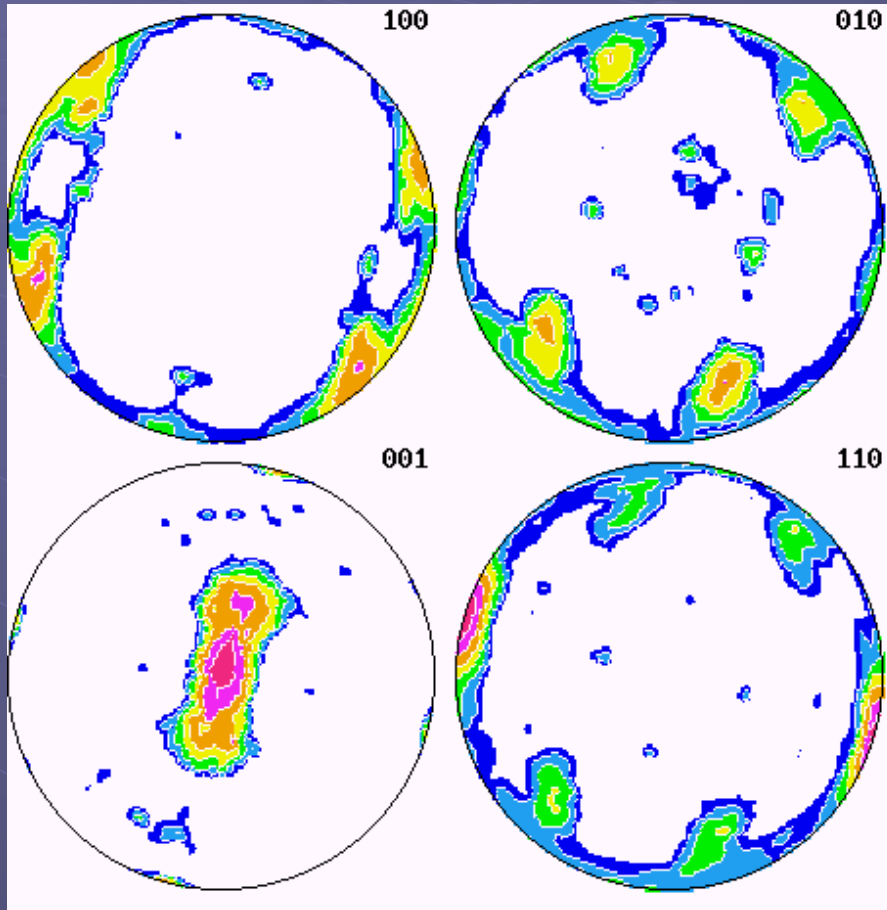
(360,90)

- Beartex
- MFDP
- Siegfried
- ◻ Strotex



Pole figure plot programs correspondences

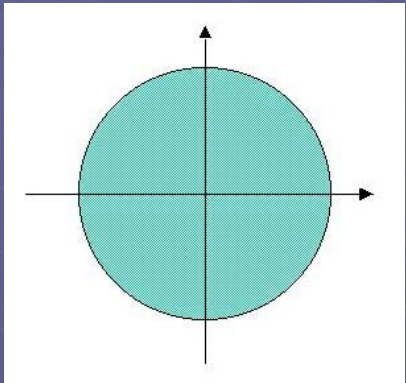
A real example



Cypraea testudinaria

Outer aragonite layer
Pnma space group

Texture types

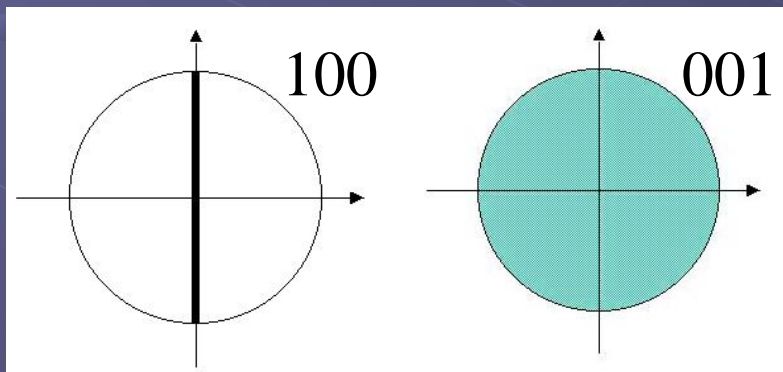


Random texture

3 degree of freedom

All $P_h(\mathbf{y})$ homogeneous

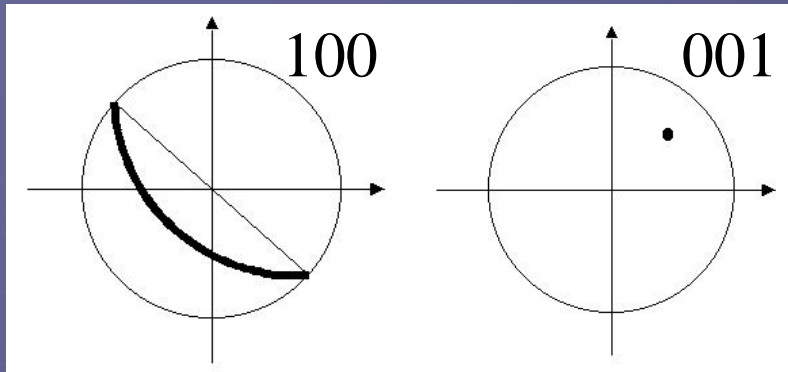
1 m.r.d. density whatever \mathbf{y}



Planar texture

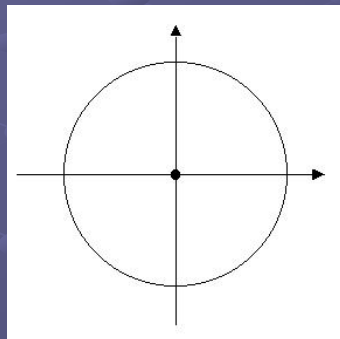
2 degree of freedom

1 $[hkl]$ at random in a plane



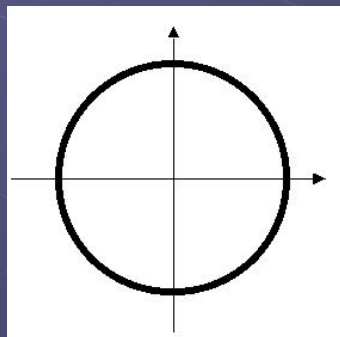
Fibre texture

1 degree of freedom
 1 $[hkl]$ along 1 y direction



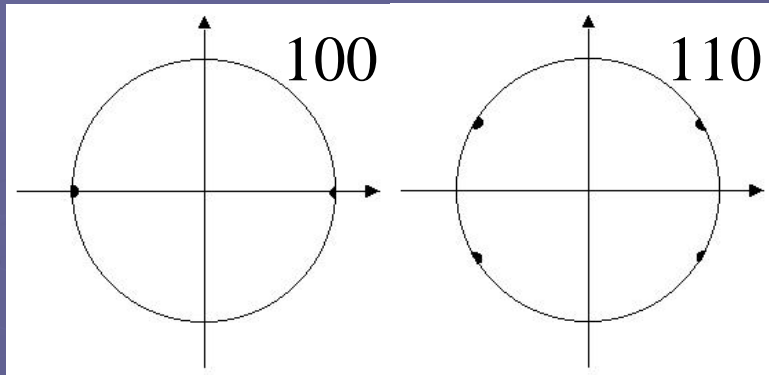
Cyclic-Fibre texture

$$\mathbf{c} // \mathbf{Z}_A$$



Cyclic-Planar texture

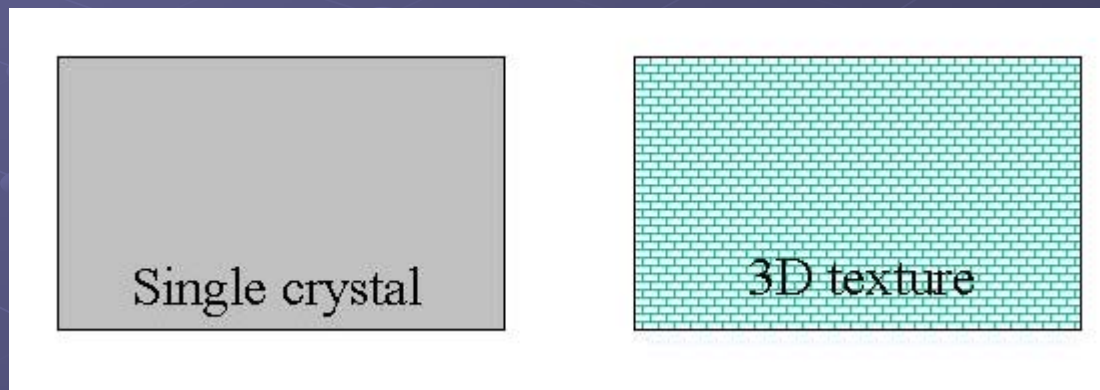
$$(\mathbf{a}, \mathbf{b}) // (\mathbf{X}_A, \mathbf{Y}_A)$$



Single crystal-like texture

0 degree of freedom

2 $[hkl]$'s along 2 y directions



Single-crystal and perfect 3D orientation not distinguished

Pole figure and Orientation spaces

Pole figure expression:

$$\frac{dV(\mathbf{y})}{V} = \frac{1}{4\pi} P_h(\mathbf{y}) d\mathbf{y}$$

$$d\mathbf{y} = \sin\vartheta_y d\vartheta_y d\varphi_y$$

$$\int_{\varphi_y=0}^{2\pi} \int_{\vartheta_y=0}^{\pi/2} P_h(\vartheta_y, \varphi_y) \sin\vartheta_y d\vartheta_y d\varphi_y = 4\pi$$

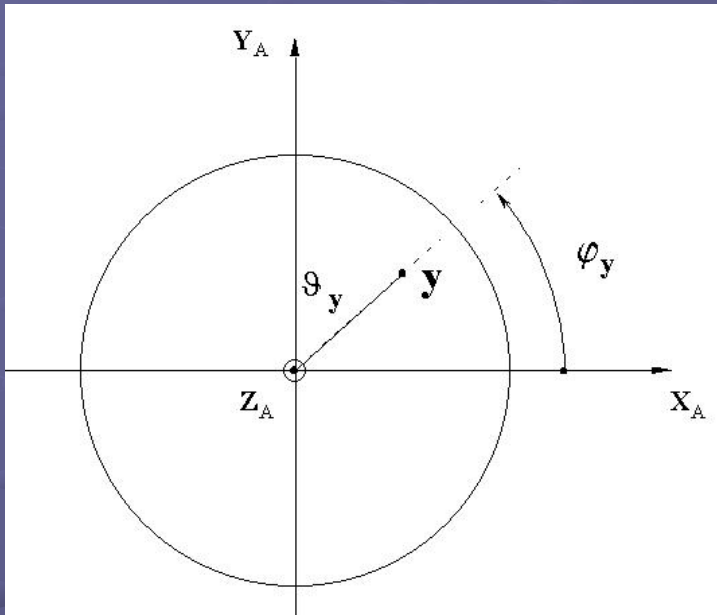
Orientation Distribution Function $f(g)$:

$$\frac{dV(g)}{V} = \frac{1}{8\pi^2} f(g) dg$$

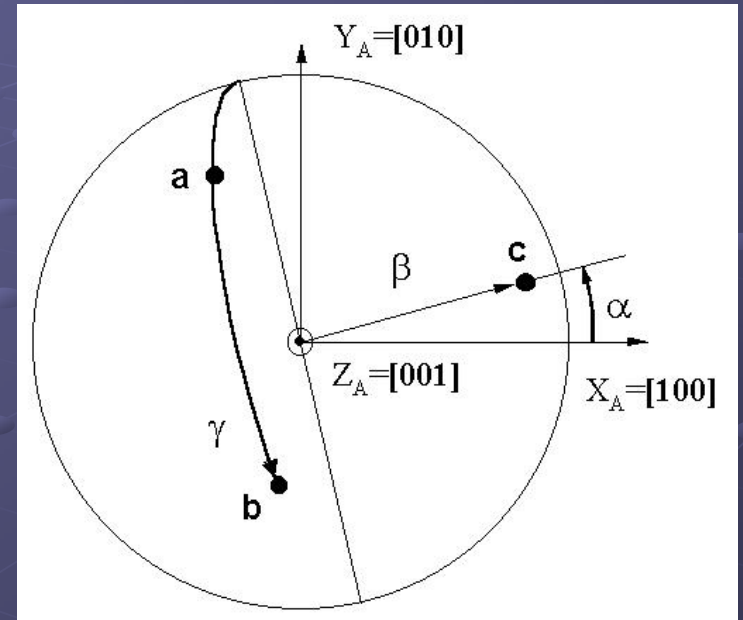
$$dg = \sin(\beta) d\beta d\alpha d\gamma$$

$$\int_{\alpha=0}^{2\pi} \int_{\beta=0}^{\pi/2} \int_{\gamma=0}^{2\pi} f(g) dg = 8\pi^2$$

From Pole figures to the ODF



Pole figure: one direction fixed in K_A



Orientation: two directions fixed in K_A

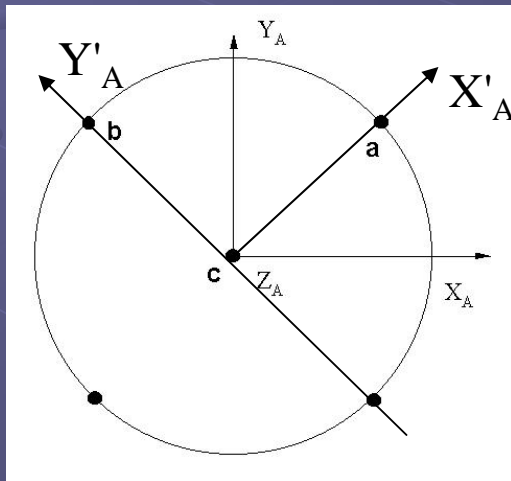
Fundamental Equation of QTA

$$P_h(\mathbf{y}) = \frac{1}{2\pi} \int_{h/y} f(g) d\tilde{\varphi}$$

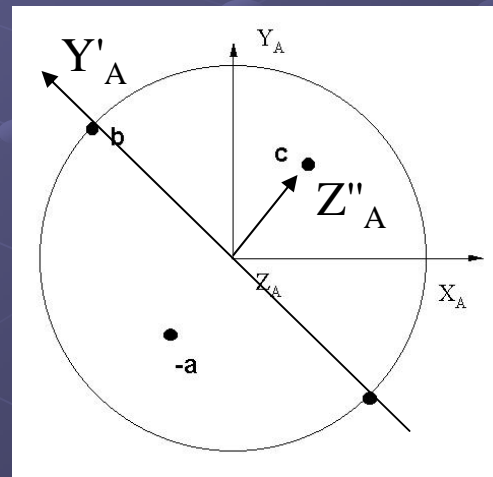
Needs several pole figures to construct the $f(g)$

Pole figures from g

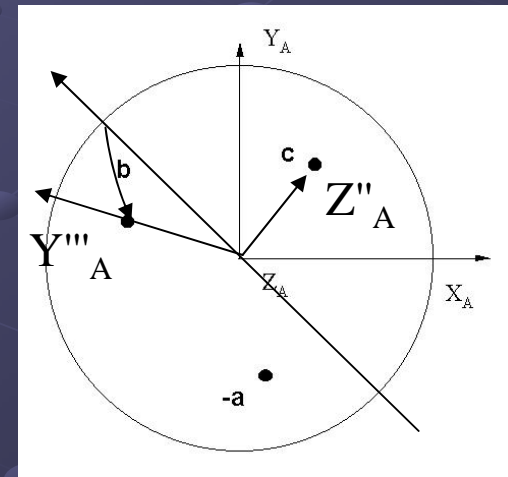
- Rotation of K_A about the axis Z_A through the angle α :
 $[K_A \mapsto K'_A]$; associated rotation $g_1 = \{\alpha, 0, 0\}$
 - Rotation of K'_A about the axis Y'_A through the angle β :
 $[K'_A \mapsto K''_A]$; associated rotation $g_2 = \{0, \beta, 0\}$
 - Rotation of K''_A about the axis Z''_A through the angle γ :
 $[K''_A \mapsto K'''_A // K_B]$; associated rotation $g_3 = \{0, 0, \gamma\}$
- finally: $g = g_1 g_2 g_3 = \{\alpha, 0, 0\} \{0, \beta, 0\} \{0, 0, \gamma\} = \{\alpha, \beta, \gamma\}$



$$g_1 = \{45, 0, 0\}$$



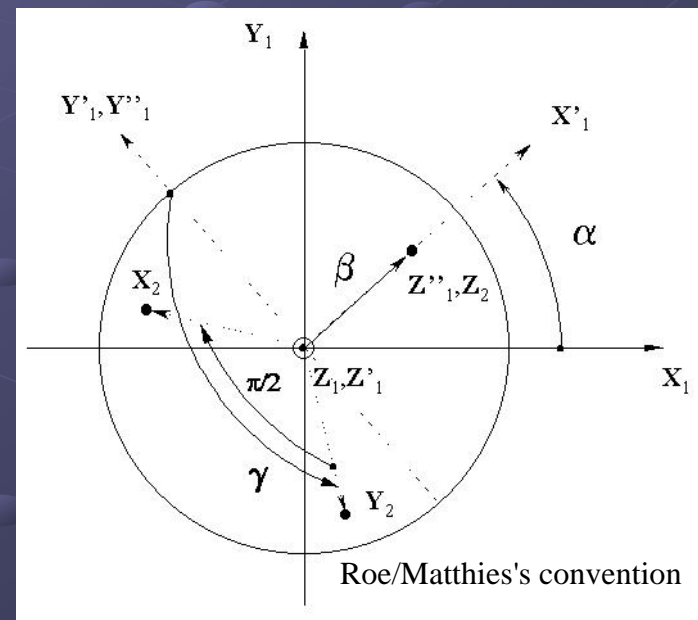
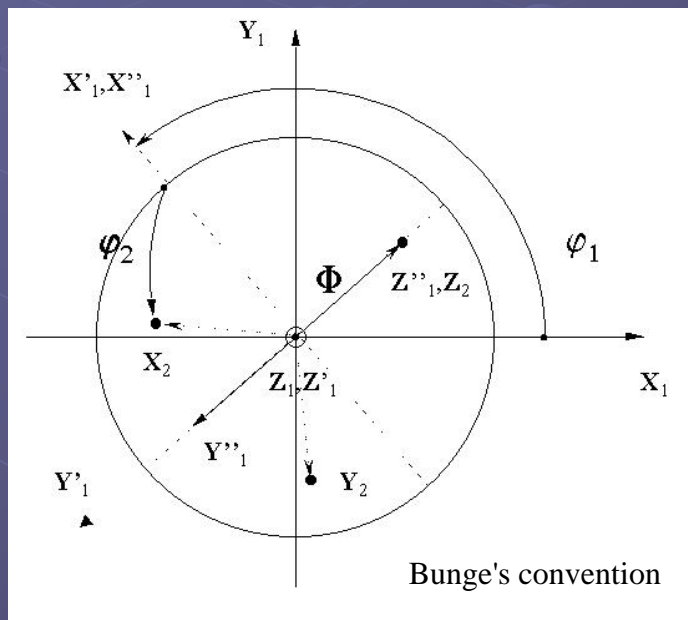
$$g_2 = \{45, 45, 0\}$$



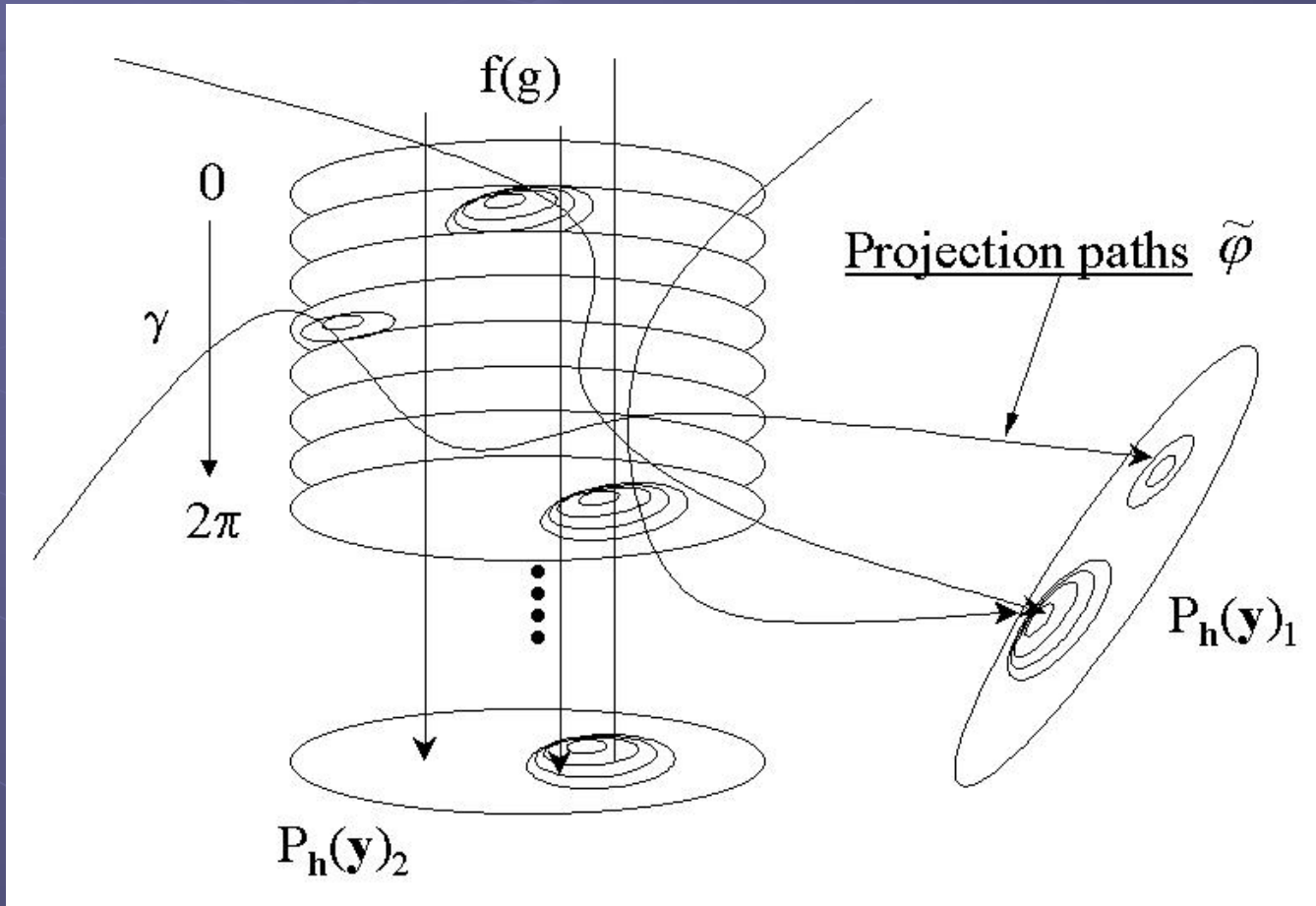
$$g_3 = \{45, 55, 45\}$$

Euler angles conventions

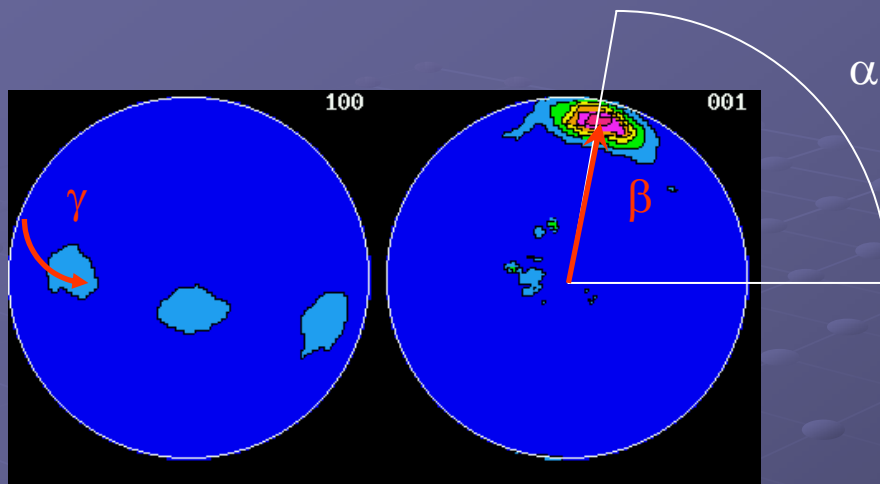
| Matthies | Roe | Bunge | Canova | Kocks |
|----------|----------|-------------------------------|---------------------------|-----------------------|
| α | Ψ | $\varphi_1 = \alpha + \pi/2$ | $\omega = \pi/2 - \alpha$ | Ψ |
| β | Θ | Φ | Θ | Θ |
| γ | Φ | $\varphi_2 = \gamma + 3\pi/2$ | $\phi = 3\pi/2 - \gamma$ | $\Phi = \pi - \gamma$ |



From $f(g)$ to the pole figures



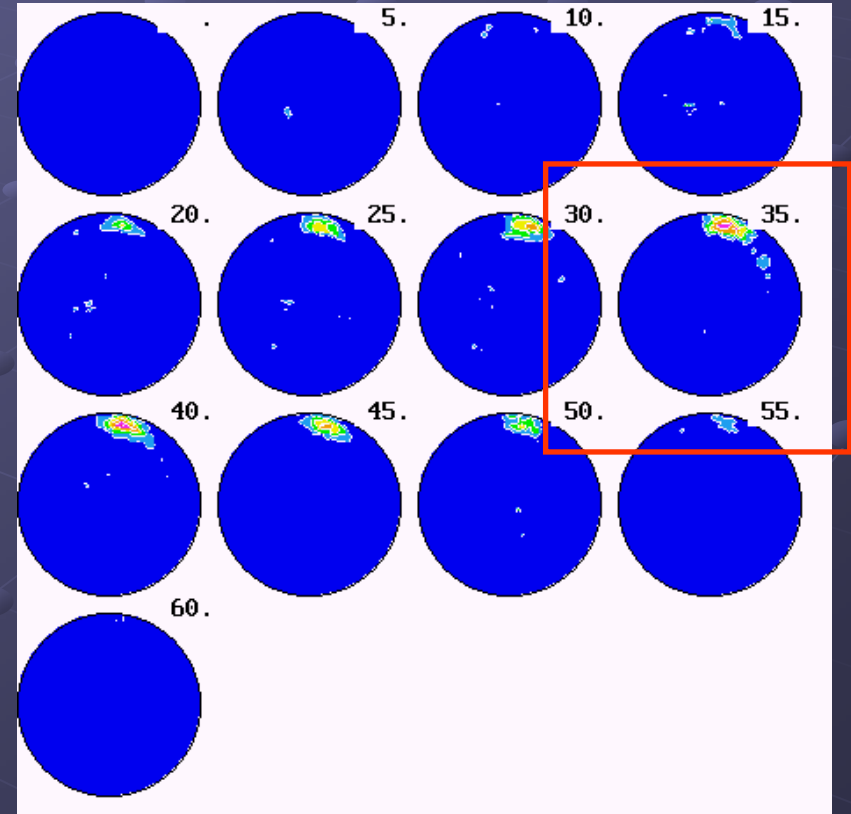
Deal with components in the ODF space



Pole figures

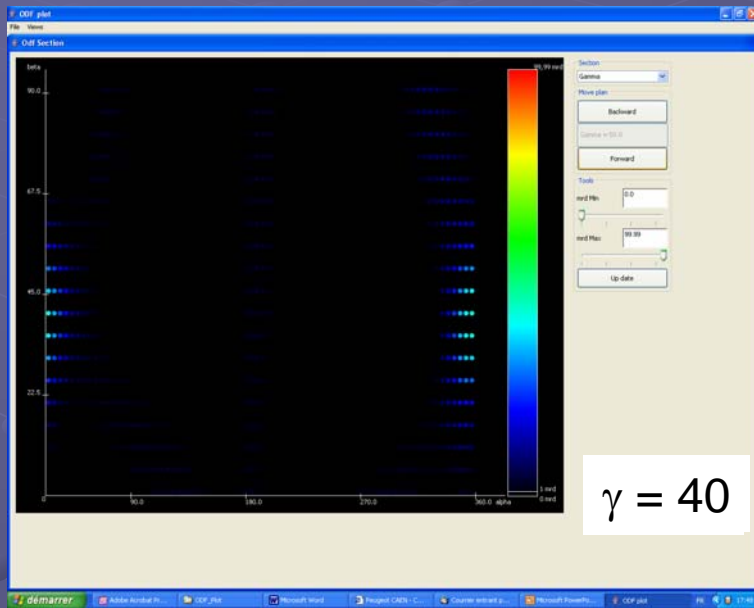
Component:
(Hexagonal system)
 $g = \{85, 80, 35\}$

ODF γ -sections

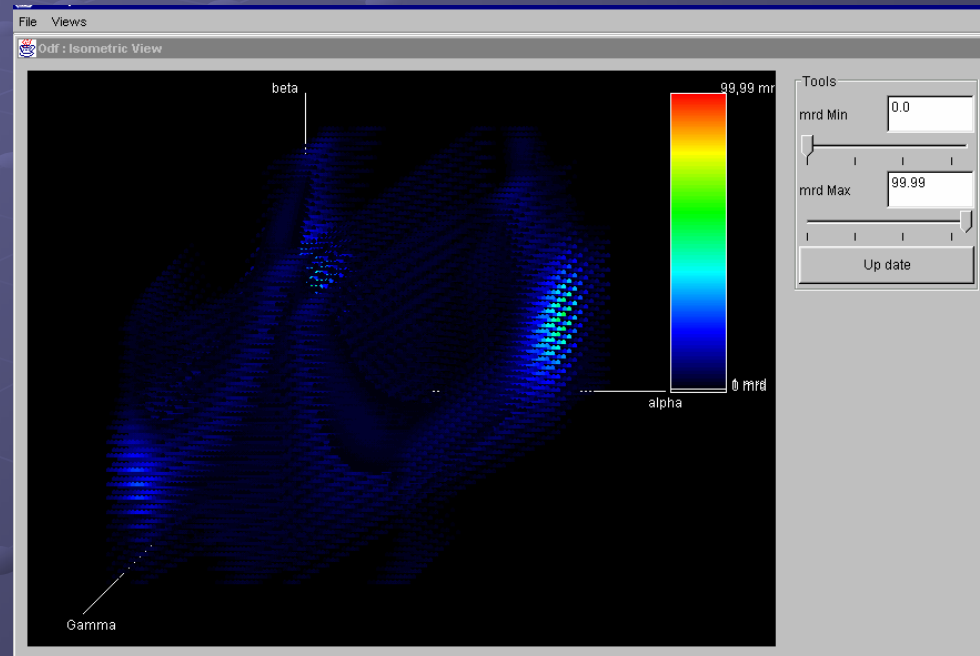


Plotting f(g)

A 3D plotting program: ODF plot



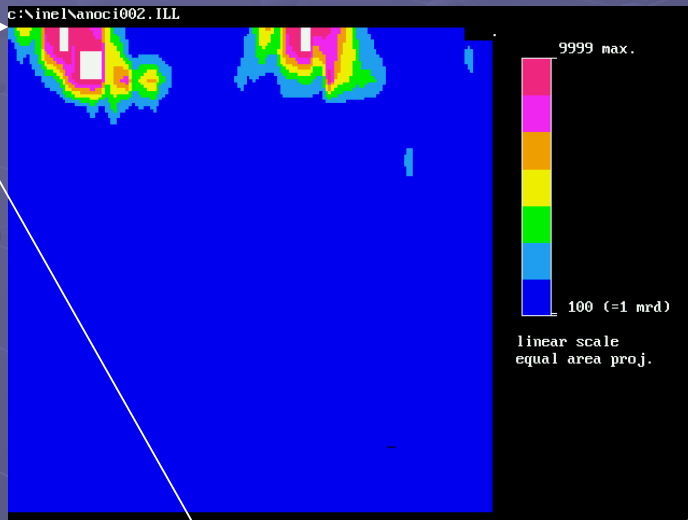
ODF sections (α , β , or γ)



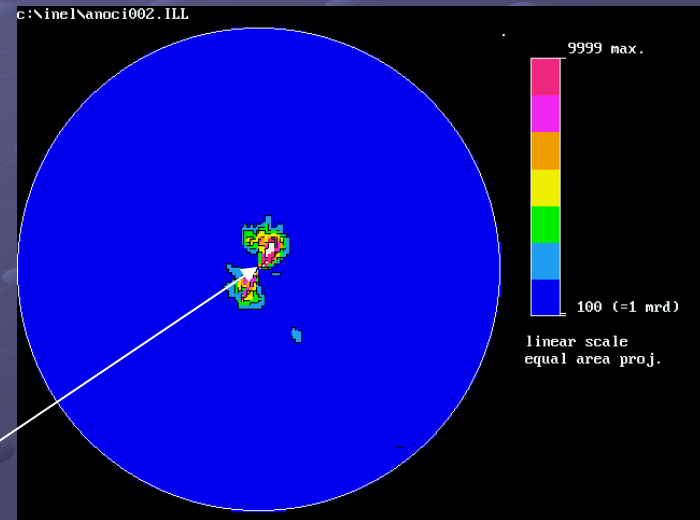
ODF 3D-isometric view

Cartesian or Polar f(g) view

Cartesian



Polar



$\beta = 0$: space deformation

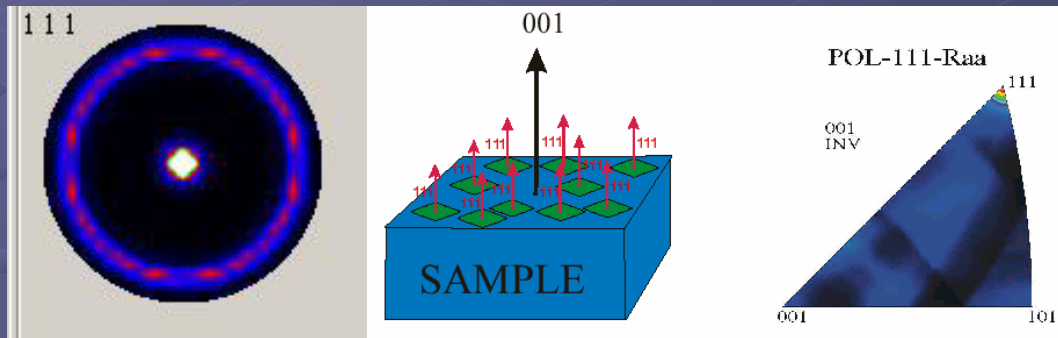
Inverse pole figures

$$P_{\mathbf{h}}(\mathbf{y}) = \frac{1}{2\pi} \int_{\mathbf{h} // \mathbf{y}} f(\mathbf{g}) d\tilde{\varphi}$$

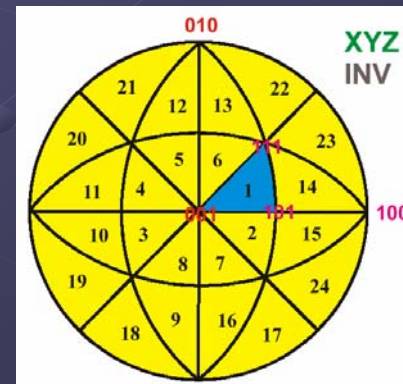
Pole figures

$$R_{\mathbf{y}}(\mathbf{h}) = \frac{1}{2\pi} \int_{\mathbf{y} // \mathbf{h}} f(\mathbf{g}) d\tilde{\varphi}$$

Inverse Pole figures



24 equivalent cubic sectors for the Inverse pole figure of a cubic system



ODF refinement

One has to invert:

$$P_{\mathbf{h}}(\mathbf{y}) = \frac{1}{2\pi} \int_{\mathbf{h}/\mathbf{y}} f(\mathbf{g}) d\tilde{\varphi}$$

- from Generalized Spherical Harmonics (Bunge):

$$f(\mathbf{g}) = \sum_{l=0}^{\infty} \sum_{m,n=-l}^l C_l^{mn} T_l^{mn}(\mathbf{g})$$

$$P_{\mathbf{h}}(\mathbf{y}) = \sum_{l=0}^{\infty} \frac{1}{2l+1} \sum_{n=-l}^l k_l^n(\mathbf{y}) \sum_{m=-l}^l C_l^{mn} k_n^{*m}(\Theta_{\mathbf{h}}\phi_{\mathbf{h}})$$

Least-squares Refinement procedure

$$\sum_{\mathbf{h}} \sum_{\mathbf{y}} [I_{\mathbf{h}}(\mathbf{y}) - N_{\mathbf{h}} P_{\mathbf{h}}(\mathbf{y})]^2 d\mathbf{y}$$

But even orders are the only available parts:

$$f^e(\mathbf{g}) = \sum_{\lambda=0(2)}^{\infty} \sum_{m,n=-\lambda}^{\lambda} C_{\lambda}^{mn} T_{\lambda}^{mn}(\mathbf{g})$$

- from the WIMV iterative process (Williams-Imhof-Matthies-Vinel):

$$f^{n+1}(g) = N_n \frac{f^n(g) f^0(g)}{\left(\prod_{h=1}^I \prod_{m=1}^{M_h} P_h^n(\mathbf{y}) \right)^{\frac{1}{IM_h}}}$$

and

$$f^0(g) = N_0 \left(\prod_{h=1}^I \prod_{m=1}^{M_h} P_h^{\text{exp}}(\mathbf{y}) \right)^{\frac{1}{IM_h}}$$

E-WIMV (Rietveld only):

with $0 < r_n < 1$, relaxation parameter,
 M_h number of division points of the integral around k ,
 w_h reflection weight

$$f^{n+1}(g) = f^n(g) \prod_{m=1}^{M_h} \left(\frac{P_h(\mathbf{y})}{P_h^n(\mathbf{y})} \right)^{r_n \frac{w_h}{M_h}}$$

- Entropy maximisation (Schaeben):

$$f^{n+1}(g) = f^n(g) \prod_{m=1}^{M_h} \left(\frac{P_h(\mathbf{y})}{P_h^n(\mathbf{y})} \right)^{\frac{r_n}{M_h}}$$

- arbitrarily defined cells (ADC, Pawlik):

Very similar to E-WIMV, with integrals along path tubes

- Vector method (Ruer, Baro, Vadon):

I linear equations for J unknown quantities:

$$\mathbf{P}_i(\mathbf{h}) = [\sigma_{ij}(\mathbf{h})] f_j$$

- Component method (Helming):

$$f(g) = F + \sum_c I^c f^c(g)$$

Gaussian component:

$$f(g, g^c) = f(\tilde{g}) = \frac{2\sqrt{\pi}}{\zeta \left\{ 1 - \exp\left(-\left(\frac{\zeta}{2}\right)^2\right)\right\}} \exp\left(-\left(\frac{\tilde{g}}{\zeta}\right)^2\right)$$

$$S = \frac{\ln 2}{1 - \cos\left(\frac{\zeta}{2}\right)}$$

$$N(S) = \frac{1}{I_0(S) - I_1(S)}$$

Evaluation of the OD coverage

Say 20 measured ($5^\circ \times 5^\circ$) complete pole figures:

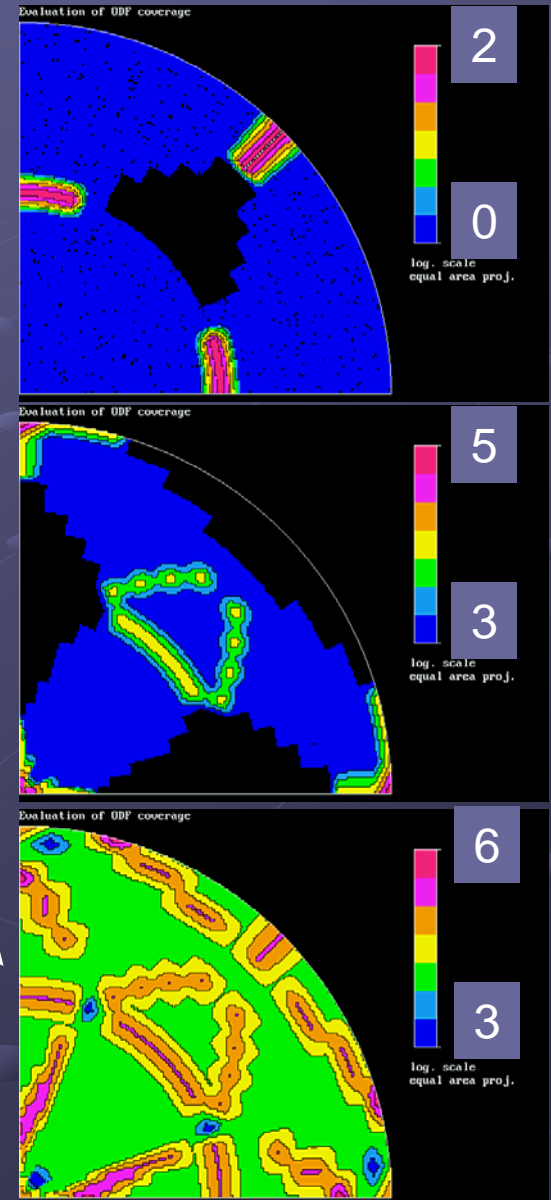
= $20 \times 1368 = 27360$ experimental points

ODF ($5^\circ \times 5^\circ \times 5^\circ$, triclinic): 98496 points to refine

{100} pole figure, measured up to $\chi = 45^\circ$:

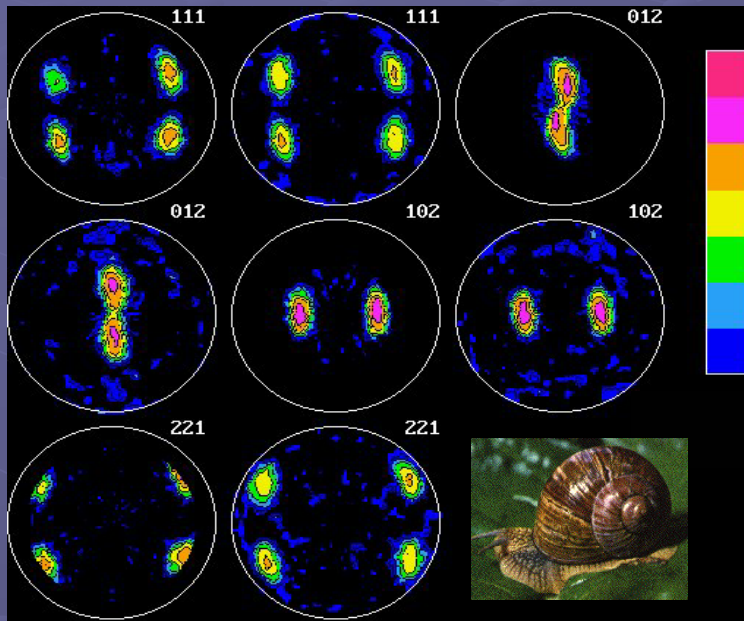
{100} + {110}, measured up to $\chi = 45^\circ$:

{100} + {110} + {111}, up to $\chi = 45^\circ$:

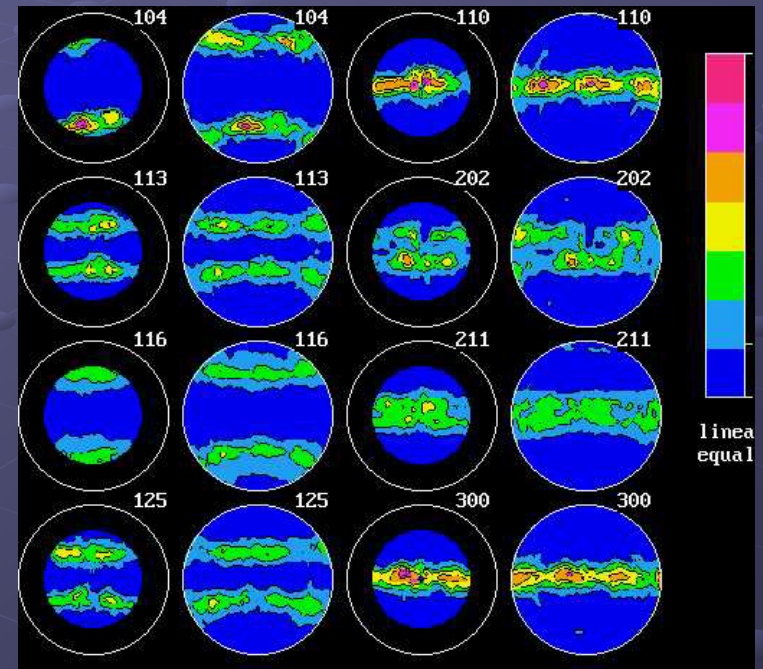


Estimators of Refinement Quality

Visual assessment



Helix pomatia (Burgundy land snail:
Outer com. crossed lamellar layer)



Bathymodiolus thermophilus (deep
ocean mussel: Outer Prismatic layer)

RP Factors:

Individual pole figures:

$$RP_x(h_i) = \frac{\sum_{j=1}^J |\tilde{P}_{h_i}^o(y_j) - \tilde{P}_{h_i}^c(y_j)|}{\sum_{j=1}^J \tilde{P}_{h_i}^o(y_j)} \theta(x, \tilde{P}_{h_i}^o(y_j))$$

$$\theta(x, t) = \begin{cases} 1 & \text{for } t > x \\ 0 & \text{for } t \leq x \end{cases}$$

$x = \varepsilon, 1, 10 \dots$

Averaged on all pole figures:

$$\overline{RP}_x = \frac{1}{I} \sum_{i=1}^I RP_x(h_i)$$

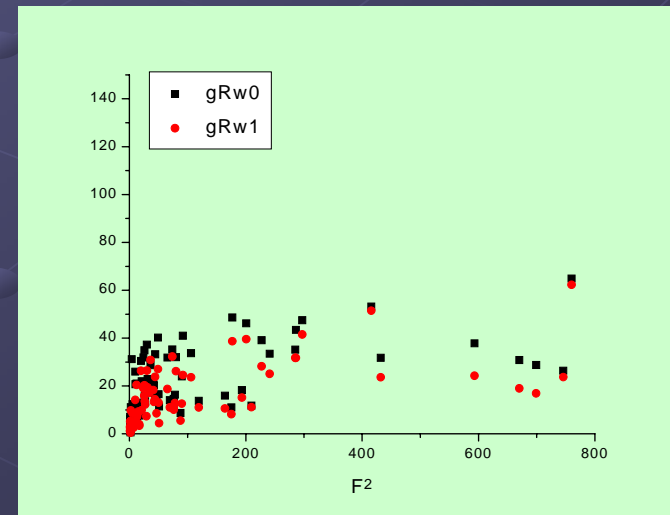
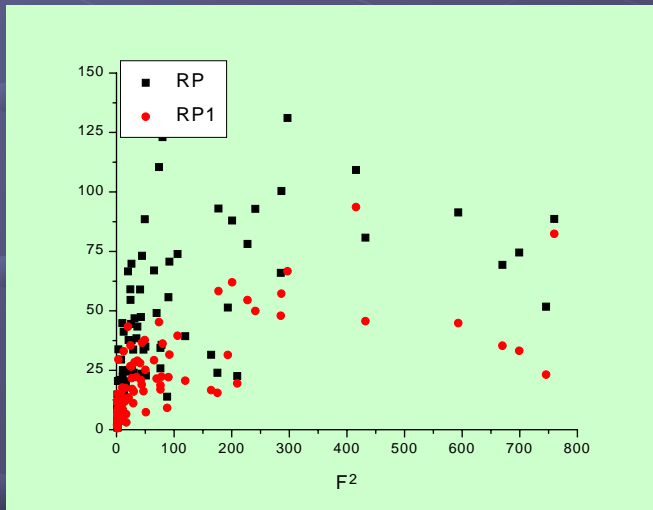
Bragg R-Factors:

$$RB_x(h_i) = \frac{\sum_{j=1}^J [\tilde{P}_{h_i}^o(y_j) - \tilde{P}_{h_i}^c(y_j)]^2}{\sum_{j=1}^J \tilde{P}_{h_i}^o{}^2(y_j)} \theta(x, \tilde{P}_{h_i}^o(y_j))$$

Weighted Rw-Factors:

$$w_{ij} = \frac{1}{\sqrt{I_{h_i}^o(y_j)}}$$

$$Rw_x(h_i) = \frac{\sum_{j=1}^J [w_{ij}^o I_{h_i}^o(y_j) - w_{ij}^c I_{h_i}^c(y_j)]^2}{\sum_{j=1}^J w_{ij}^o{}^2 I_{h_i}^o{}^2(y_j)} \theta(x, \tilde{P}_{h_i}^o(y_j))$$



Texture strength estimators

ODF Texture Index:

$$F^2 \in]1, \infty[\quad > 1 \text{ m.r.d}^2 \\ = 1: \text{ powder} \\ = \infty: \text{ single crystal}$$

$$F^2 (\text{m.r.d.}^2) = \frac{1}{8\pi^2} \sum_i f^2(g_i) \Delta g_i$$

Discrete OD

$$F^2 = 1 + \sum_{\lambda=2}^L \left[\frac{1}{2\lambda+1} \right] \sum_{m=-\lambda}^{\lambda} \sum_{n=-\lambda}^{\lambda} |C_{\lambda}^{mn}|^2$$

Continuous ODF

Pole figures Texture Index:

$$J_h^2 = \frac{1}{4\pi} \sum_i [P_h(\mathbf{y}_i)]^2 \Delta \mathbf{y}_i$$

Texture Entropy:

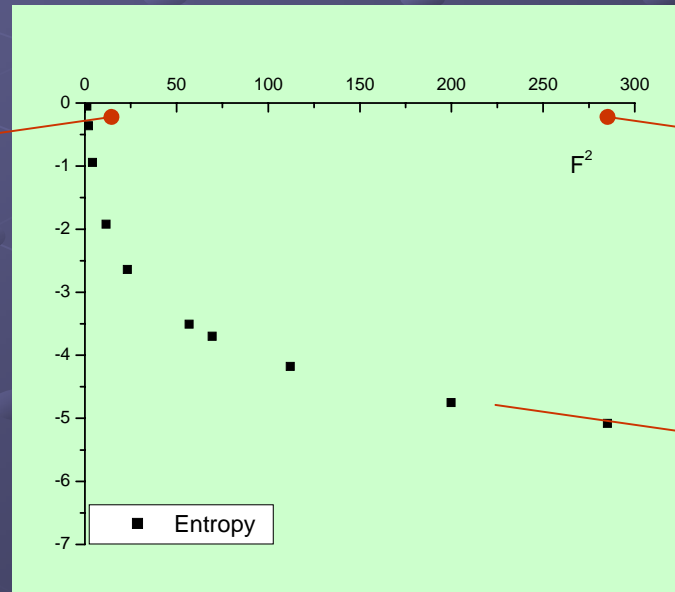
$$S \in [0, -\infty[\quad \leq 0$$

= 0: powder
= $-\infty$: single crystal

$$S = \frac{-1}{8\pi^2} \sum_i f(g_i) \ln[f(g_i)] \Delta g_i$$

S - F²:

Fon +
smooth
texture component(s)

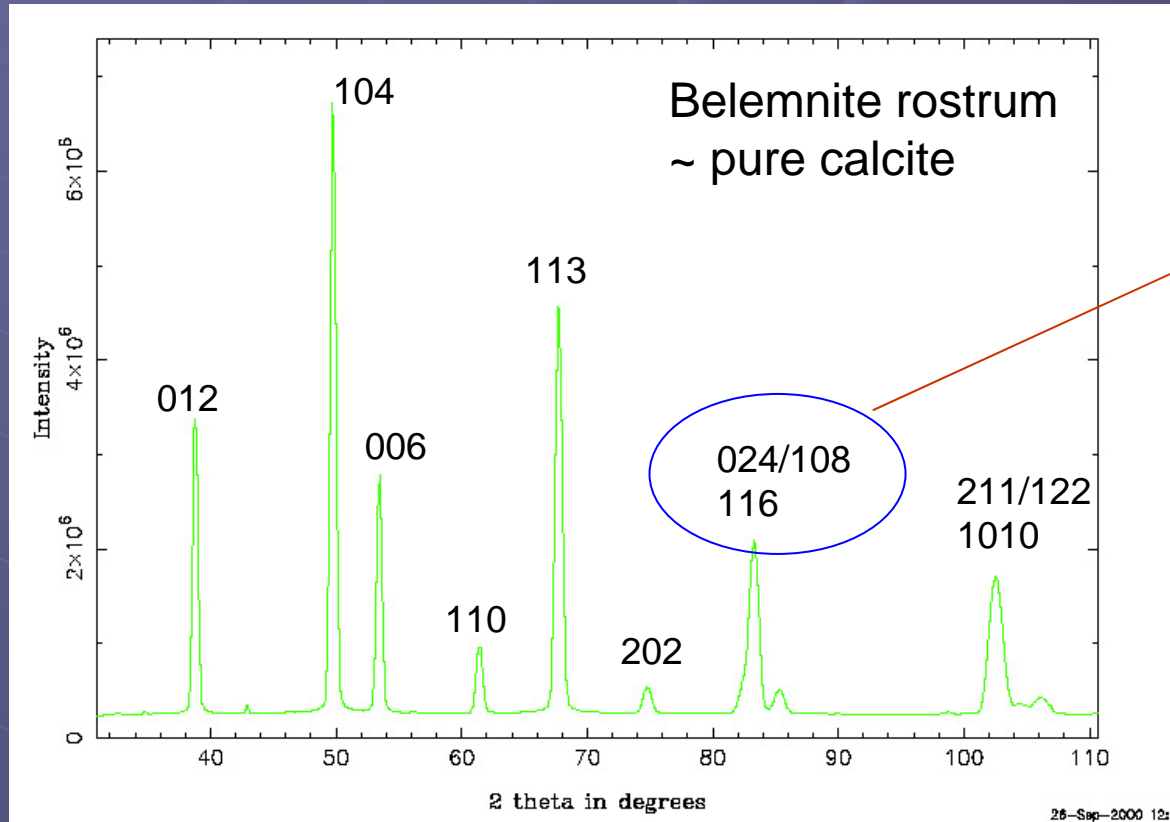


Fon +
Dirac-like
texture component

Lower bound:
Fon = 0

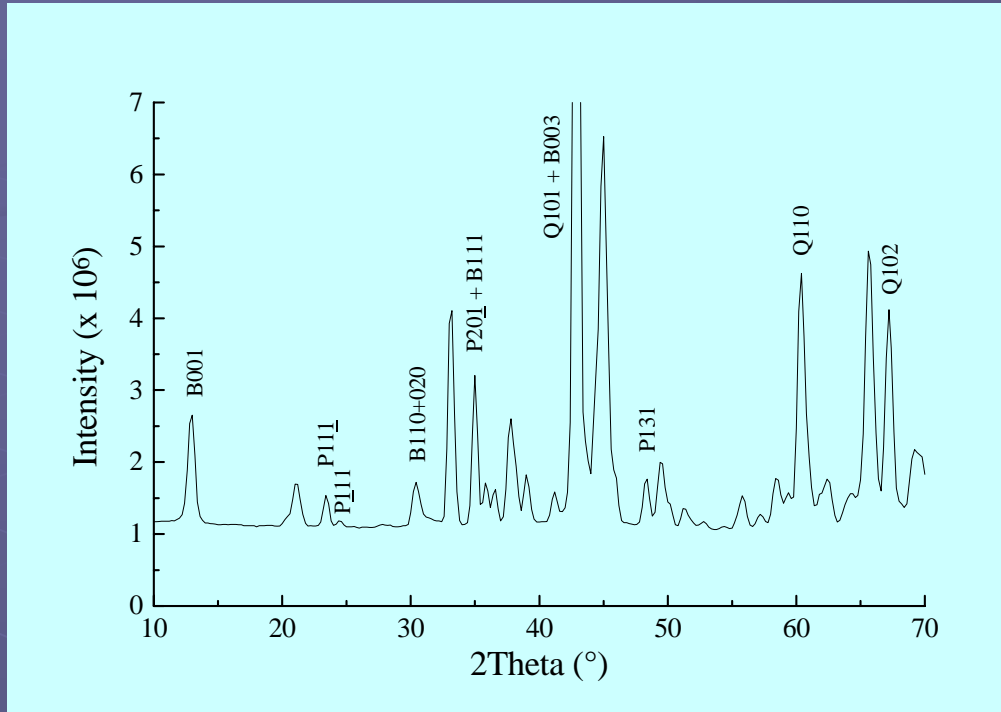
Why needing combined analysis

- Solve the peak-overlap problems (intra- and inter-phases)



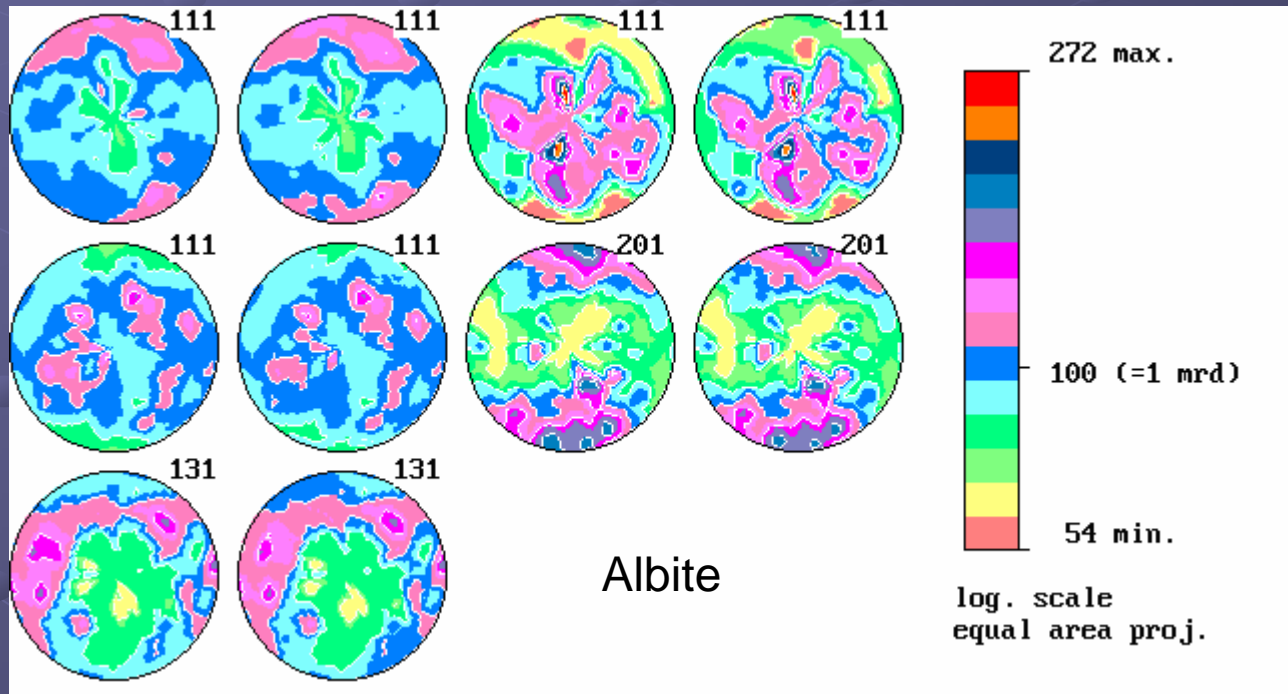
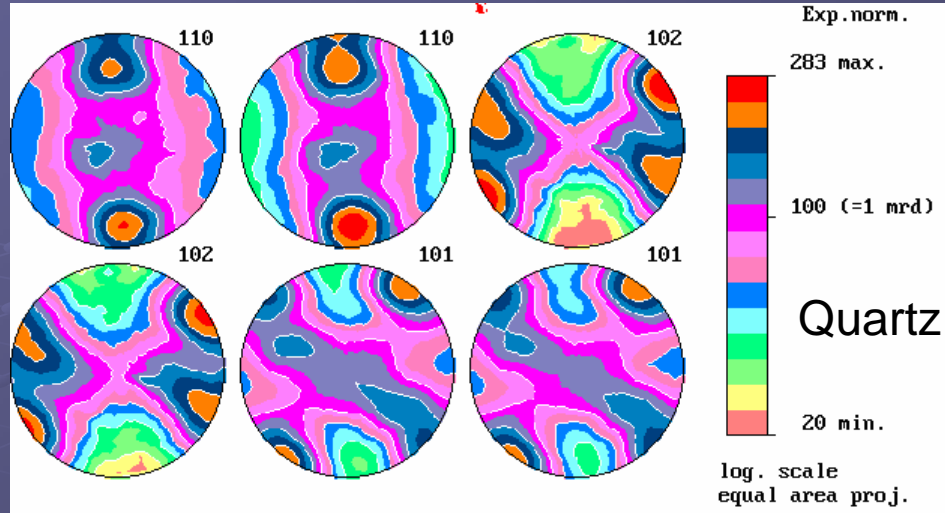
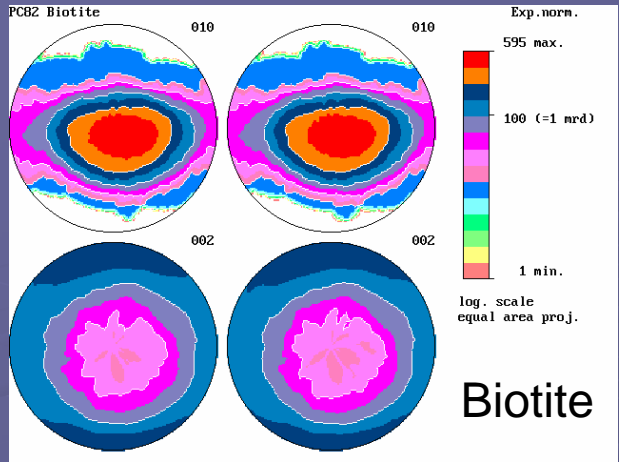
Resolved during
ODF refinement

Polyphased Mylonite (Palm Canyon, CA)

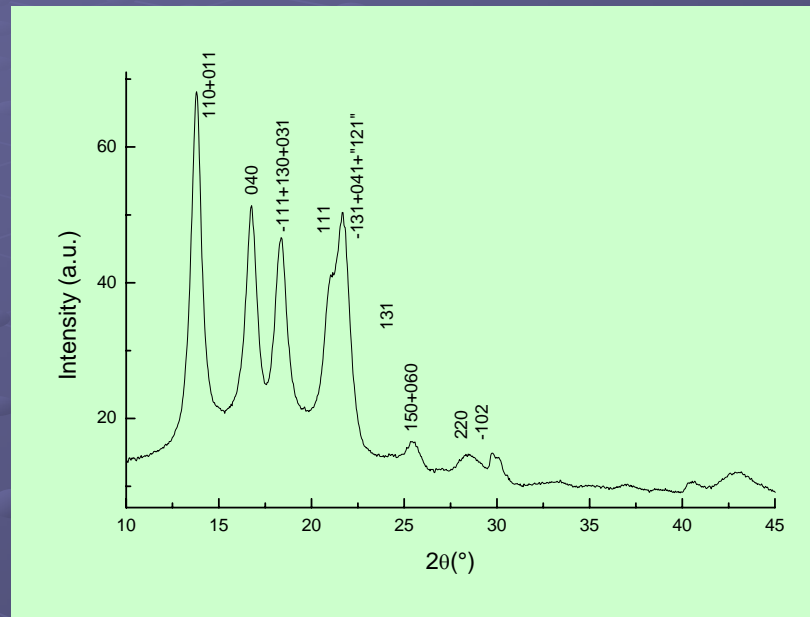


Using 0D detector
hardly manageable

| PC 82 mylonite | Biotite | Quartz | Albite | Anorthite | K-spar |
|------------------------|---------|--------|--------|-----------|--------|
| Composition (weight %) | 9.0 | 24.2 | 31.7 | 17.4 | 14.1 |
| Space group | C2/m | R3 | C-1 | | |



Plasma-treated polypropylene films



Large broadening + overlaps + amorphous phase

- Don't want or can't powderise your sample:
 - . Rare: Ice from deep cores, meteorite rocks ...
 - . Expensive: high-tech materials
 - . Impossible: hard materials, polymers, thin structures ...
- Decreases instrument time:
 - . $5^\circ \times 5^\circ$ grid = 1368 points / pole figure
 - . ODF: needs as much pole figures as possible
- Access to other parameters:
 - . crystal sizes, micro-strains, stacking faults + twins (QMA)
 - . residual strains and stresses (QSA)
 - . Structure determination
 - . Phase proportions (QPA)
 - . Thicknesses, roughnesses (XRR)

- Avoid false minima due to parameter correlation:

- . phase and texture
- . Structure and texture
- . Structure and strains
- . Thickness and phase
- ...

- Benefit of these correlation to access "true" values

Textured materials: between powder and single-crystal,
angular discrimination

- Easier to practice !